Wetlands (2026) 46:68
https://doi.org/10.1007/s13157-026-02074-3

ORIGINAL RESEARCH ARTICLE

Role of Typha latifolia, Juncus balticus, and Root-Associated Microbial Communities in Naphthenic Acid Removal from Oil Sands Process-Affected Water

Amy-lynne Balaberda[1] · Julius Eyiuche Nweze[2] · Ian J. Vander Meulen[3] · Jason M. E. Ahad[4] · John V. Headley[3] · Étienne Yergeau[2] · Christine Martineau[5] · Dani Degenhardt[1]

Received: 18 November 2025 / Accepted: 6 May 2026 / Published online: 15 June 2026
© Crown 2026

Abstract

Oil sands process-affected water (OSPW), a by-product of surface mining in Alberta, Canada, contains persistent and toxic naphthenic acid fraction compounds (NAFCs). Constructed wetland treatment systems are a promising biological approach for reducing NAFCs, yet the role of plant-microbe-substrate interactions remains underexplored. In this study, greenhouse mesocosms containing coarse sand tailings (CST) and either OSPW or reverse osmosis (RO) water were planted with *Typha latifolia*, *Juncus balticus*, or left unplanted. Plant growth did not differ between mesocosms with OSPW and RO, however *T. latifolia* health declined due to an aphid infestation. Plants influenced substrate and water chemistry by reducing salinity, alkalinity, and ions such as Ca and K, while tissues showed distinct uptake patterns, with *J. balticus* enriched in Fe, S, and P, and *T. latifolia* elevated in Ca and K. Plants also enhanced NAFC removal, increasing from 16% in unplanted mesocosms to 32% with *J. balticus* and 40% with *T. latifolia*. Isotopic analyses indicated preferential removal of bitumen-derived NAFCs, providing an independent line of evidence for OSPW attenuation. Despite reduced health, *T. latifolia* achieved the highest NAFC attenuation, suggesting species-specific mechanisms, likely including microbial stimulation. *T. latifolia* roots had a higher diversity and were enriched in putative hydrocarbon degraders (*Burkholderiaceae*), while *J. balticus* hosted putative Fe-cycling taxa (*Gallionellaceae*). Putative hydrocarbon degraders were also detected under RO, indicating latent bioremediation potential. These results demonstrate that plant identity may mediate CWTS performance, likely through effects on chemistry and microbial communities, highlighting the importance of targeted species selection for OSPW treatment.

Keywords Constructed wetland treatment systems · Naphthenic acid fraction compounds · Oil sands process-affected water · Plant-microbe interactions · *Typha latifolia* · *Juncus balticus*

Introduction

The Athabasca oil sands region (AOSR) of Alberta, Canada, contains one of the largest proven petroleum reserves on earth, estimated at 1.7 to 1.8 trillion barrels-of-oil equivalent (Natural Resources and Canada 2015). These deposits are often shallow enough to be surface-mined, but extraction of mined bituminous ore produces large volumes of oil sand process-affected water (OSPW). For every barrel of oil produced, the hot water extraction process has historically required 2 to 4 barrels of fresh water (Natural Resources and Canada 2015). Considerable volumes of OSPW have therefore accumulated on the landscape, where approximately 1.4 billion m^3 of tailings is estimated to be held in regional

✉ Dani Degenhardt
Dani.Degenhardt@NRcan-RNcan.gc.ca

1 Natural Resources Canada, Canadian Forest Service, Edmonton, Canada

2 Institut national de la recherche scientifique, Laval, Canada

3 Environment and Climate Change Canada, National Hydrology Research Centre, Saskatoon, Canada

4 Natural Resources Canada, Geological Survey of Canada, Québec, Canada

5 Natural Resources Canada, Canadian Forest Service, Québec, Canada

tailings pits, of which ~ 400 Mm^3 is estimated to be OSPW (Alberta Energy and Regulator 2024). Raw or untreated OSPW is toxic (Li et al. 2017), and contains high levels of metals, salts, and organic compounds through continued cycling and reuse in the extraction process (Hussain and Stafford 2023; Masliyah et al. 2008). The characterization of OSPW has been shown to cause toxic effects on mammals (Gurney et al. 2005; Rogers et al. 2002), invertebrates (Lari et al. 2016), amphibians (Melvin and Trudeau 2012; Robinson et al. 2023), fish (Kavanagh et al. 2012; Marentette et al. 2015; Van den Heuvel et al. 2012), and plants (Armstrong et al. 2010).

Toxicity in OSPW has been strongly linked to naphthenic acids (NAs) (Hughes et al. 2017; Morandi et al. 2015; Verbeek 1995). NAs are a naturally occurring group of complex carboxylic acids that are described under the formula $C_nH_{2n}{}_{+Z}O_2$ (n is the number of carbon atoms; Z is a negative even integer corresponding to the unsaturation of a molecule) (Brient et al. 2004). Adverse outcomes related to NAs are proposed to stem from their amphipathic behaviours as surfactant-like molecules (Lipnick 1993; Roberts 1991), which suggests that NAs would cause toxicity through cellular narcosis (Frank et al. 2009). This is further reinforced by subsequent toxicity evaluations, where increasing molecular weight (i.e., increasing amphipathic characteristics) leads to increasing toxicity in OSPW-derived NAs (Hughes et al. 2017; Scarlett et al. 2012).

As analytical methods have improved in resolution and specificity, it has become clear that there are a broader variety of naphthenic acid fraction compounds (NAFCs) present in the mixture of organic acids (Headley et al. 2011, 2013). These NAFCs follow the general formula $C_nH_{2n+Z}O_xN_\alpha S_\beta$, where n represents the number of carbon atoms, z similarly summarizes unsaturation, X denotes the count of oxygen atoms, α denotes the count of nitrogen atoms, and β denotes the count of sulphur atoms (Vander Meulen et al. 2021a). This broader class of compounds subsumes classical NAs, while also allowing for technically non-naphthenic acids (e.g., aromatic acids), as well as a variety of heteroatom-containing (e.g., nitrogen and sulphur-containing) compounds that might otherwise be excluded. Despite the strong link between OSPW acute toxicity and O_2-compounds (i.e., mostly classical NAs), recent work has suggested that other classes of compounds also contribute appreciably to adverse outcomes (Leshuk et al. 2024), providing reason to look for broadly non-targeted analyses to characterize NAFCs.

Because of the toxicity of OSPW, a zero-discharge policy is enforced to safeguard both aquatic and terrestrial ecosystems (AEPA, 2024a). While stakeholders have shown interest in the potential release of treated OSPW, regulatory guidelines are not yet developed. A wide range of physical, chemical and biological technologies have been investigated to treat OSPW, including coagulation/flocculation, adsorption, membrane and reverse-osmosis systems, advanced oxidation, photodegradation, and a variety of biological approaches (Quinlan and Tam 2015). While many of these approaches can remove specific constituents effectively at small scales, questions remain about their scalability, energy requirements, consumables requirements, and therefore cost-effectiveness when applied to the large volumes of wastewater produced by the oil sands industry (Kannel and Gan 2012; Scott et al. 2020). For example, electro-oxidation and/or ozonation systems require ongoing chemical and/or electrical inputs (Abdalrhman et al. 2020; Zhang et al. 2019), which can contribute to higher per-liter treatment costs. In contrast, bioremediation-based strategies such as constructed wetland treatment systems (CWTS) offer a low-energy, cost-efficient and publicly acceptable alternative. The treatments provided by CWTS harness natural processes to reduce concentrations and toxicity of NAFCs and other OSPW constituents and can be scaled to treat large volumes while maintaining relatively low operating costs (Reis et al. 2023; Rodgers and Castle 2008).

CWTS operate through an interplay of physical, chemical and biological mechanisms. Abiotic mechanisms can include settling, filtration, sorption, precipitation, photodegradation and chemical oxidation, while biotic processes include microbial biodegradation, plant-mediated biotransformation, and phytoaccumulation. Biodegradation and sorption have been identified as key drivers for the removal of complex organics like NAFCs (Cancelli and Gobas 2022, 2024). Mechanistic investigations show that NAFCs can adsorb to soil substrates (Medeiros et al. 2023) dependent on associated ionic strength and water chemistry parameters (Hanneseth et al. 2006; Janfada et al. 2006), can be taken up and assimilated into plant tissues (Alberts et al. 2021), or otherwise transformed by a combination of photolytic (Challis et al. 2020; McMartin et al. 2004) and biodegradative processes (Reis et al. 2023; Whitby 2022). Mesocosm and field CWTS studies treating OSPW have demonstrated measurable NAFC attenuation over weeks to months, with reported reductions varying by design, residence time, and plant presence (Ahad et al. 2018; Ajaero et al. 2018, 2020; Cancelli and Gobas 2022; Hendrikse et al. 2018; McKenzie et al. 2014; Simair et al. 2021; Trepanier et al. 2023, 2025). Certain emergent macrophytes perform reliably in OSPW systems: *Juncus balticus*, *Typha latifolia*, and *Carex aquatilis* have shown good survival and functional performance in experimental OSPW wetlands, making them practical candidates for CWTS plantings (Zhao et al. 2024).

Plant-microbe partnerships are central in hydrocarbon breakdown (Correa-García et al. 2018) and are therefore critical in determining CWTS success for OSPW treatment. Microbial communities carry out the enzymatic

transformations that mineralize or detoxify NAFCs and other organic contaminants. Plants influence these microbial processes through rhizodeposition: root exudates (organic acids, sugars, and secondary metabolites) serve as labile carbon sources that stimulate heterotrophic degraders, alter local pH, and modulate redox microenvironments, thereby enhancing biodegradation rates and altering sorption dynamics (Alberts et al. 2021; Reis et al. 2023). In turn, microbes can promote plant health by degrading toxic compounds in the rhizosphere, producing phytohormones, and mitigating stress responses, which is especially valuable where NAFC toxicity can inhibit root growth (Reis et al. 2023).

Root-associated microorganisms are particularly important during phytoremediation of organic compounds (Khan et al. 2013). Previous studies have examined root-associated microbiomes of wetland species, including *T. latifolia* in natural or artificial wetlands (Martínez-Martínez et al. 2023; Pietrangelo et al. 2018; Zapata-Morales et al. 2020). However, the temporal dynamics of root microbial communities in *J. balticus* and *T. latifolia*, and how these dynamics influence plant-specific differences in nutrient uptake, microbial interactions, and NAFC removal, remain poorly understood. In particular, limited information on how variation in microbial colonization between plant species affects the mechanisms that drive NAFC attenuation or overall plant health is available, constraining efforts to optimize phytoremediation strategies for large-scale treatment of OSPW.

Mesocosm experiments provide a controlled, intermediate-scale platform to address these knowledge gaps and bridge the scale between laboratory assays and field systems. By controlling water type, substrate, plant assemblage and exposure duration, mesocosms allow mechanistic inquiry into the processes that govern NAFC attenuation, ion dynamics and plant health under realistic but repeatable conditions (Balaberda et al. 2025). This study used *T. latifolia*, *J. balticus* and unplanted controls in mesocosms receiving either OSPW or reverse osmosis (RO) water to evaluate performance in treating NAFCs within OSPW. The overlying water chemistry, soil/substrate chemistry, and plant survival and growth were analyzed, and NAFCs were characterized using high-resolution Orbitrap mass spectrometry and stable carbon isotope analysis. The microbial community in root samples of both plant species was profiled, due to the importance of root-associated microorganisms during phytoremediation of organic compounds. This mesocosm study provides experimental proof-of-concept under realistic OSPW treatments and, by comparing species-specific effects, addresses the gap in understanding how plant identity influences CWTS performance and microbial community dynamics.

Materials and Methods

Experimental Design and Setup

This experiment was conducted in a greenhouse at the Northern Forestry Centre in Edmonton, Alberta, using coarse sand tailings (CST) and OSPW collected from Kearl oil sands mine (Imperial Canada Ltd.).

Each mesocosm (polypropylene; 50.8 cm height × 33.02 cm width × 129.54 cm length; volume: 248.09 L) was filled with 20 cm (85.6 L) of CST. A 25 cm water column (106.9 L) of either OSPW or RO water was maintained above the substrate. The mesocosms operated as surface-flow closed-loop systems. Water was pumped from 159 L reservoir tanks into each mesocosm at ~20 mL/min, running intermittently every 10 min, which cycled at approximately 28.8 L/day. System design and operational procedures followed standard mesocosm protocols (Balaberda et al. 2025).

T. latifolia and *J. balticus* seeds were collected from natural stands within seed zones DM1.3 (Dry Mixedwood) and CM1.1 (Central Mixedwood), respectively. Seedlings were grown in peat plugs for three to five months prior to transplanting. The plants were fertilized three times weekly with water-soluble fertilizer (24-8-16, Miracle-Gro All purpose Plant Food).

Twelve individuals of either species were transplanted into each mesocosm. At the time of transplanting, *T. latifolia* ranged from 61 to 162 cm in height (average of 120.8 ± 17.0 cm), and *J. balticus* ranged from 45 to 115 cm (average of 70.5 ± 12.0 cm). To acclimate the plants to the mesocosm system, RO water was used to slowly raise the water level over two months to the target depth of 25 cm, followed by another two months of system acclimation. During this 129-day acclimation period, fertilizer (10-10-10, Golfgreen All Purpose Garden Fertilizer) was added as needed to address nutrient deficiencies. Algal growth resulting from fertilization was managed by flushing the system with RO water once, approximately half-way through the 129-day acclimation phase.

The experiment followed a randomized block design using two greenhouse bays. A total of six treatments were tested, each with four replicates ($n = 24$ mesocosms): RO water (Unplanted), OSPW (Unplanted), OSPW + *J. balticus*, RO water + *J. balticus*, OSPW + *T. latifolia*, RO water + *T. latifolia* (Fig S1). The experiment lasted 89 days, stopping approximately mid-way through the 23rd four-day cycle, with each cycle designed to fully exchange the free water volume in the mesocosm with the reservoir.

Greenhouse conditions were maintained at approximately 20 °C during the day and 10 °C at night, with a 16-hour photoperiod. These temperature and light conditions were selected to approximate typical growing season

conditions in this region, ensuring physiologically relevant plant growth and microbial activity while maintaining controlled experimental conditions. RO water was added to the reservoirs for all mesocosms as needed to compensate for losses due to evapotranspiration and to maintain consistent water levels.

General Chemistry and Plant Health Analyses

General chemistry parameters for the substrate and water were analyzed at the beginning (prior to OSPW addition) and the end of the experiment by Element Materials Technology (Edmonton, AB, Canada). The analysis for the substrates included pH, electrical conductivity (EC), sodium absorption ratio (SAR), major ions and metals concentrations (e.g., calcium (Ca), magnesium (Mg), sodium (Na), potassium (K), chloride (Cl), sulfate (SO_4), nitrate (NO_3), nitrite (NO_2), iron (Fe), manganese (Mn). The analysis of the water included pH, EC, hardness, total dissolved solids (TDS), total alkalinity, and major ions. Additional water parameters (pH, dissolved oxygen, salinity, oxidation reduction potential (ORP), and conductivity) were monitored at the end of every cycle (4 days) with a YSI® Professional Plus Multiparameter. Soil redox potential was measured with a portable millivolt (mV) meter and silver chloride electrodes (Fisherbrand Accumet Epoxy Body Mercury-Free Reference Electrode CAT #13–620-858) using platinum tip probes installed into each mesocosm (Faulkner et al. 1989; Huddleston and Rodgers 2008).

Plant parameters were measured at the end of each 4-d cycle. Plant heights (cm), aboveground plant biomass (g), and visual observations were used as indicators to determine plant health and vigor. Vigor (i.e., live vs. dead plant tissue) was scored for each individual plant on a 1–7 scale: 1 = 100% dead, 2 = 70–99% dead, 3 = 40–70% dead, 4 = 20–40% dead, 5 = 10–20% dead, 6 = 1–10% dead, 7 = 0% dead. To quantify major ion concentrations (i.e., trace metals, total nitrogen, and phosphorus) in plant tissue, the entire aboveground biomass for each mesocosm was collected at the end of the experiment and sent to Element Materials Technology (Edmonton, AB, Canada) for analysis.

Sample Preparation and High-Resolution MS Analysis of NAFCs

Samples were shipped from the Northern Forestry Center (Edmonton, Alberta) to the National Hydrology Research Center (Saskatoon, Saskatchewan) overnight in coolers on ice. After samples were received, samples were transferred to a 4 °C refrigerator and kept in the dark until extractions could be performed (within 1 week).

Water samples were prepared for mass spectrometry analysis by an established solid-phase extraction (SPE) procedure (Headley et al. 2002). Sample aliquots were measured to ~100 mL (with exact volumes recorded). To prepare SPE cartridges for analysis, 6 mL/200 mg ENV+ cartridges (Biotage, Charlotte, NC, USA) were first rinsed with 1 column volume (6.0 mL) of MilliQ water (≥18.2 MΩ), then with 1 column volume (6.0 mL) of "Optima" LC/MS-grade methanol (Fisher Scientific Canada, Edmonton, Alberta, Canada), and columns were subsequently re-conditioned with 6–12 mL of MilliQ water to condition cartridges prior to sample loading. Just prior to beginning extractions, samples were pH-adjusted to ≤2 by adding excess (~2 mL) formic acid (≥98%; Fisher Scientific, Edmonton, Alberta, Canada). Acidified samples were extracted through preconditioned SPE cartridges through polytetrafluoroethylene (PTFE) transfer lines at 2–3 mL/min. Following comprehensive extraction of sample aliquots, samples were de-salted by adding 1 column volume (6 mL) of MilliQ water drawn through at 2–3 mL/min. De-salted cartridges were dried by drawing a gentle vacuum through the SPE extraction manifold for ~15 min. Analyte extracts were subsequently eluted from desalted, dried cartridges by the addition of 6.0 mL of "Optima" LC/MS-grade methanol under gravity. Sample extracts were dried completely under a gentle flow of N_2 (5.0-grade; Linde Canada, Saskatoon, Saskatchewan, Canada) in clean glass culture vials partially immersed in a water bath at ~40 °C. Extracts in culture vials were reconstituted with 50:50 acetonitrile: H_2O with 0.1% (v/v) NH_4OH by vortexing residues with the solvents for 20–25 s each. Once they were reconstituted, sample extracts were transferred to clean, labelled 2.0 mL amber LC/MS autosampler vials. To monitor ongoing method performance and laboratory background, method blanks (i.e., SPE extractions of MilliQ water) were carried out with each batch following the same protocol, but provided no cause for background corrections.

Non-targeted analyses for NAFCs were carried out using a ThermoFisher Scientific Orbitrap LTQ Velos Elite mass spectrometer via loop injection in negative ionization mode with resolution set to 240,000 (as measured by peak width at half height at 400 m/z). Sample extracts were handled via an autosampler to make 5 µL injections, where data were collected from a 1-minute total ion chromatogram following the injection. Instrument conditions were as follows: sheath gas flow 25 (arbitrary units); auxiliary gas flow 5 (arbitrary units); sweep gas 1 (arbitrary units); spray voltage −2.90 kV, S lens radio frequency level at 67%, heater temperature 50 °C; capillary temperature 275 °C. Injections were made using an isocratic mobile phase composition of 50:50 acetonitrile: H2O with 0.1% (v/v) NH_4OH to match extract compositions. Detected m/z values were dynamically

recalibrated using a lock mass value provided by a lab-ubiquitous background ion previously identified as n-butyl benzenesulfonamide ($C_{10}H_{15}NO_2S[-H]^-$; −212.07507 m/z).

Quantification of NAFCs was achieved using an external standard strategy, where a 5-point curve of 10, 25, 50, 75, and 100 mg/L was re-acquired every 10–12 sample injections to ensure ongoing method linearity and uniform instrument response. Preparation of the in-house NAFC standard has been previously reported elsewhere (Headley et al. 2002; Rogers et al. 2002). As with all NA and NAFC quantification methods, a lack of available reference standards limits this quantification to being semi-quantitative (Hindle et al. 2023), and therefore values reported here can only be internally compared to samples processed and quantified by the same method.

All qualitative data (i.e., formulae) from Orbitrap-MS was pre-processed using XCalibur 2.2 software (Thermo-Fisher Scientific, Waltham, MA, USA) to remove irrelevant regions from the total ion chromatograms (i.e., pre- and post-injection data regions). Trimmed data were imported into Composer64 version 1.5.6 software (Sierra Analytics, Modesto, CA, USA) for *de novo* formula assignments (<3 ppm) made over a mass range of 100 195 to 500 according to the following multi-pass algorithm: allowed atom counts in pass 1 included #C 0–50, 196 #H 0–150, #N 0–3, and #O 0–10; in pass 2 #C 0–50, #H 0–150, #O 0–3, #S 0–5; pass 3 #C 0–50, #H 0–197 150, #N 0–3; pass 4 #C 0–50, #H 0–150, #N 0–3, #O 0–3, #S 0–3. Allowed assignments were restricted 198 to those with ≤3 ppm mass error.

Carboxyl-Group Targeted Carbon Isotope Analysis

Stable carbon isotope analysis targeting the CO_2 generated by pyrolytic decarboxylation ($\delta^{13}C_{pyr}$) is a technique that can distinguish OSPW-derived from non-bitumen, plant-derived NAFCs (Ahad et al. 2012, 2013, 2020; Gibson et al. 2025; Trepanier et al. 2023, 2025). Following a protocol adapted from Ahad et al. (2012), 1 L of water collected in fluorinated HDPE bottles (Thermo Fisher Scientific, Mississauga, ON, Canada) was acidified to pH 4.5 and extracted with loose Strata-X-A SPE sorbent (Phenomenex, Torrance, CA, USA) pre-rinsed with methanol and MilliQ water. Approximately 100 mg of sorbent was used per litre of water. The samples were vortexed in large glass beakers for 2 h using a magnetic stir bar. The sorbent was then filtered from the aqueous phase under vacuum using glass fibre filters and NAFCs were eluted with 10% formic acid in methanol and pure methanol. To maximize recoveries, water samples were treated a second time using another 100 mg sorbent. The extracts containing NAFCs were combined and then evaporated to dryness under ultrahigh purity N_2, weighed, and re-dissolved in methanol. Extraction blanks carried out using 1 L of MilliQ water and put through the same procedure as described above yielded no detectable background NAFCs.

Small aliquots corresponding to around 1 mg of extract were transferred by syringe into a 40 µL rigid silver capsule, dried, and sealed with pliers prior to isotopic analysis. The $\delta^{13}C_{pyr}$ values were determined at the Delta-Lab of the Geological Survey of Canada (Québec, QC, Canada) using a thermal conversion elemental analyzer (TC/EA) interfaced with a Delta Plus XL isotope ratio mass spectrometer (Thermo Fisher Scientific, Bremen, Germany). Samples were decarboxylated at 750 °C in a pyrolysis reactor and analyzed against CO_2 calibrated to international carbonate standards (Oztech Trading Corp., Safford, AZ). Based on replicate standard and sample analyses, the precision achieved for $\delta^{13}C_{pyr}$ analyses was ±0.3‰.

Microbial Sampling and Analyses

Sample Preparation

Root samples were collected from *T. latifolia* and *J. balticus* for microbial community analysis. Sediment (CST) samples were initially collected; however, DNA yields were consistently low, preventing reliable sequencing. Therefore, only root-associated microbial communities were analyzed in this study.

Immediately after their collection from mesocosms, roots were quickly cleaned with tap water to dislodge root-bound soil, rinsed with deionized water, pat dried, and transferred to a 50 mL Falcon tube prior to snap-freezing in a dry ice-ethanol bath. Samples were shipped on dry ice to the Laurentian Forestry Center (Québec City, Canada) where they were stored in a −80 °C freezer until further processing. Prior to DNA isolation, 100 mg of fine frozen roots were transferred to a 2.0 mL Safe-Lock microtube (Eppendorf) containing a 5 mm stainless steel bead (Qiagen) and ground to a fine powder using the TissueLyser II (Qiagen) at 26 Hz for ≥2 × 45 s, with snap-freezing by immersing the tubes in liquid nitrogen between grinding cycles.

DNA Isolation, Library Preparation and Sequencing

DNA isolation was performed with the DNeasy PowerSoil Pro kit (Qiagen). Volumes of 800 µL of solution CD1 plus 0,2 µL of a dilution (10 ng/µL) of exogenous DNA of *Thermus thermophilus* (strain HB8; 27634D-5, ATCC) were mixed and added into microtubes containing the fine root powder. These mixtures were then transferred into PowerBead Pro tubes and vortexed for a few seconds. Samples were then thoroughly homogenized using the TissueLyser II at 25 Hz for 2 × 5 min and centrifuged for 1 min at 15,000

× *g* prior to DNA isolation with QIAcube instruments (program PowerSoil Pro, including IRT; Qiagen) following the manufacturer's instructions. DNA concentration was measured using the Qubit dsDNA Broad Range assay kit (Life Technologies) and Qubit 3.0 fluorometer (Thermo Fisher Scientific). DNA extracts were diluted to 6 ng/µL with 10 mM Tris pH 8.0 solution using the QIAgility automated system (Qiagen). Library preparation was performed by the Centre d'expertise et de services, Génome Québec (Montréal, Canada). Libraries were generated from 100 ng of DNA, using the NEBNext Ultra II DNA Library Prep kit for Illumina (New England BioLabs) as per the manufacturer's recommendations and sequenced on a 25B flow cell (Illumina) on a NovaSeq X Plus instrument (Illumina). A phiX library was used as a control and mixed with libraries at 1% level.

Microbial Community Profiling

Taxonomic assignment of sequence reads was performed using SingleM (v0.18.3) (Woodcroft et al. 2024) with 35 bacterial and 37 archaeal single-copy marker genes, using default settings. This approach targets the short, 20 amino acid regions (encoded by 60 nucleotides) within single-copy marker genes. The "SingleM pipe" subcommand produced OTU tables and Genome Taxonomy Database (GTDB) taxonomic profiles. The "SingleM summarise" command was then used to compute relative abundances by species-by-site and convert to unifrac format. Among the unifrac files generated for marker genes, the file with default ribosomal protein (S3.5.ribosomal_protein_S2_rpsB) data was selected for bacteria and archaea.

Data Analysis and Visualization

All data analyses were conducted in R (Core Team 2024). Statistical analysis of soil chemistry, water chemistry and plant health metrics were performed using glmmTMB and tidyverse (Bolker et al. 2009; Zuur et al. 2010). A summary of the different modelling approaches used for each parameter can be found in Table S1.

Soil chemistry parameters were analyzed using generalized linear mixed models (GLMMs) with plant species, water type, and sampling date (and their interactions) as fixed effects and mesocosm as a random effect. Models were generally fitted with a Gaussian distribution and a dispersion term structured by date, except for SO_4, which was modelled using a Gamma distribution with a log link due to non-normal residuals.

Water chemistry parameters were analyzed using generalized linear models (GLMs) with plant species, water type, and their interaction as fixed effects. Only the final sampling time point was analyzed, as initial (0 d) samples represented the acclimation with RO water. Dispersion structures were adjusted when necessary (e.g., Ca ~ Species, Na ~ Water) to improve model fit. One replicate mesocosm in the Unplanted RO water treatment exhibited abnormal chemistry which was associated with rust formation and was thus excluded from statistical analysis for soil and water chemistry.

Plant height was analyzed separately for *T. latifolia* and *J. balticus* with GLMMs assuming a Gaussian distribution including day, water type, and their interaction as fixed effects, and mesocosm as a random effect. Plant tissue ion concentrations were analyzed using GLMs with a Gaussian distribution with plant species, water type, and their interaction as fixed effects, with log transformation for Cu and Fe. Tissue ion concentrations were further analyzed using principal component analysis (PCA) with the prcomp() function in R (Core Team 2024).

Model fit was assessed using residual diagnostics (*DHARMa*) (Harting 2024), and significance of fixed effects was evaluated with Type III Wald chi-square tests (*car*) (Fox and Weisberg 2019). Where significant effects were detected, pairwise comparisons were performed using estimated marginal means (*emmeans*) and Tukey-adjusted p-values (Lenth et al. 2025).

Aboveground biomass was analyzed separately for each plant species using one-way ANOVA (*aov*) with water type as the fixed factor. Residuals were checked for normality using histograms, Q-Q plots, and Shapiro-Wilk tests, confirming assumptions were met.

For comparison of high-resolution mass spectral identifications of NAFC mixture constituents, data were ordinated via PCA using R's built-in prcomp() function (Core Team 2024). Base peak-normalized abundance for mass spectral values were filtered to exclude formulae that occurred in <3 samples, followed by Pareto-scaling (Ivosev et al. 2008; Van Den Berg et al. 2006) and then using a single-value decomposition strategy implemented by the default prcomp function built into R.

Isotopic signatures for OSPW samples were analyzed for significant differences using GLMMs with plant species and sampling date (and their interactions) as fixed effects and mesocosm as a random effect. Models were fitted with a Gaussian distribution and a dispersion term structured by date. Model fit was assessed using residual diagnostics (*DHARMa*) (Harting 2024), and significance of fixed effects was evaluated with Type III Wald chi-square tests (*car*) (Fox and Weisberg 2019). Where significant effects were detected, pairwise comparisons were performed using estimated marginal means (*emmeans*) and Tukey-adjusted p-values (Lenth et al. 2025).

Data from SingleM were imported into R to construct a genus-level OTU matrix, and alpha diversity was

evaluated using Richness, Shannon, and Simpson indices. Prior to hypothesis testing, the distribution of each metric was assessed using the Shapiro-Wilk test and homogeneity of variance was evaluated with Levene's test. Because Shannon and Simpson indices deviated from normality, non-parametric Wilcoxon rank-sum tests were applied for group comparisons, whereas Richness (normally distributed) was analyzed using Student's t-tests and adjusted using Benjamini–Hochberg (BH) correction. Analyses were performed within each plant species (OSPW vs. RO) and between plant species under OSPW exposure. Results were visualized with boxplots stratified by these variables.

Beta diversity was assessed in R using Bray-Curtis dissimilarity on normalized genus abundance data from SingleM. Non-metric multidimensional scaling (NMDS) was performed to ordinate samples in two dimensions. Statistical differences in community composition were tested using permutational multivariate analysis of variance (PERMANOVA) (adonis2) to assess centroid (mean composition) shifts, and PERMDISP to evaluate group dispersion (variability). These analyses were performed for water type effects within each plant species, and for plant species effects within the OSPW treatment. All tests used 999 permutations. Hierarchical clustering was performed using the UPGMA algorithm in SingleM with jackknife support values.

Results and Discussion

Substrate Chemistry

The CST substrate consisted predominantly of sand (98.0% ± 0.0), with minor proportions of silt (1.5% ± 0.6) and clay (0.5% ± 0.6). Iron concentrations were relatively high and variable before the experiment (1,900 ± 245 mg/kg), but all other metals were well below provincial remediation guideline values at the final sampling event (AEPA, 2024b) (Table S2).

The GLMM showed that most soil chemistry parameters (pH, EC, SAR, Ca, Mg, Na, Cl, and SO_4) increased significantly over time ($p < 0.05$), independent of plant type or water treatment (main effect of Date; Table S3). Among these, Na, Cl, SO_4, EC, and SAR were also strongly affected by water type, with higher concentrations in OSPW mesocosms compared to RO controls ($p < 0.05$). In contrast, Ca, Mg, and K did not differ significantly between water types. Plant species also influenced substrate chemistry, with significant species × sampling date interactions for Ca, Mg, and SO_4 (Table S3). By the final sampling, soils from *T. latifolia* mesocosms contained higher Ca, Mg, and SO_4 concentrations than *J. balticus* ($p < 0.05$), but consistently lower K ($p < 0.05$). The differing behaviour of K in the CST of *T. latifolia* mesocosms may reflect *T. latifolia*'s known high K uptake (see Sect. 3.3).

Overall, the observed changes in soil chemistry reflect both mineral dissolution from substrate and plant-specific influences. Soil redox potential remained consistently above 50 mV in all treatments, indicating oxidizing conditions. Therefore, chemical changes were not driven by reductive dissolution but by mineral weathering and ion release from CST. For example, the increase in Ca across all treatments (Table 1), including the unplanted RO mesocosms, suggests CST remained a continuing source of Ca even after the 129-d acclimation period. Parallel increases in Mg and SO_4 support continued mineral dissolution, with OSPW additions amplifying SO_4 accumulation relative to RO controls (Table 1).

pH dynamics reflected both abiotic buffering and biological activity. Across all treatments, including unplanted RO mesocosms, pH increased over time, likely due to carbonate dissolution in CST and other buffering processes. However, pH remained consistently lowest in *T. latifolia* treatment. Notably, these mesocosms started below the provincial guideline range (AEPA, 2024b) but increased within acceptable levels by the final sampling, though still lower than other treatments. This pattern may be consistent with root-mediated acidification, where oxygen release into the rhizosphere enhances microbial oxidation, producing protons (H^+) and CO_2 that lower pH (Ma et al. 2022). Lower pH in *T. latifolia* treatment was accompanied by higher concentrations of Ca, Mg, and SO_4 (Table 2), consistent with increased mineral weathering, cation exchange and sulfur oxidation. These strong effects relative to *J. balticus* align with *T. latifola*'s larger footprint in the mesocosm and more extensive root system, which release more oxygen and exudates than *J. balticus* (Wießner et al. 2002), stimulating microbial activity and amplifying rhizosphere acidification despite the reduced plant health observed (Sect. 3.3).

Plant uptake likely contributed to element-specific trends, as seen in the depletion of K in *T. latifolia* relative to *J. balticus*. Increases in Na, Cl, EC, and SAR in OSPW treatments confirm that salinity accumulation was driven by OSPW inputs. However, both EC and SAR remained within the "good" category under provincial guidelines (AEPA, 2024b). Together, these results show that OSPW predictably increased salinity, but plant roots also influenced ion mobilization and soil pH. This highlights the combined roles of substrate weathering, water chemistry, and vegetation in shaping soil conditions.

Table 1 Physiochemical and inorganic properties of coarse sand tailings (CST) in oil sands process-affected water (OSPW) and reverse osmosis (RO) treatments. Initial samples (0 d) were taken prior to OSPW addition, final samples were taken after 89 d. Values represent mean ± standard deviation ($n=4$). "n.d." refers to no data available

			RO Treatment		OSPW Treatment	
	Parameters	Units	Initial	Final	Initial	Final
J.balticus	pH		6.45 ± 0.88	7.35 ± 0.91	6.45 ± 0.41	7.05 ± 0.62
	SAR		0.28 ± 0.10	0.38 ± 0.05	0.30 ± 0.08	3.42 ± 0.56
	EC	*dS/m*	0.26 ± 0.07	0.46 ± 0.12	0.22 ± 0.03	0.81 ± 0.15
	Calcium	*mg/kg*	8.05 ± 3.64	18.92 ± 6.45	6.47 ± 1.45	14.62 ± 6.00
	Magnesium	*mg/kg*	2.48 ± 1.21	5.42 ± 1.24	1.95 ± 0.70	5.38 ± 1.87
	Sodium	*mg/kg*	2.75 ± 0.96	4.50 ± 0.58	2.75 ± 1.50	38.00 ± 11.75
	Potassium	*mg/kg*	4.25 ± 1.26	3.25 ± 1.71	4.25 ± 1.89	5.00 ± 2.00
	Chloride	*mg/kg*	4.75 ± 0.96	5.75 ± 1.26	4.50 ± 2.38	10.00 ± 3.46
	Sulfate-SO_4	*mg/kg*	32.08 ± 14.40	60.25 ± 28.17	27.65 ± 7.46	116.58 ± 43.34
	Nitrate + Nitrite-N	*mg/kg*	1.12 ± 0.25	n.d.	1.12 ± 0.25	n.d.
T.latifolia	pH		5.75 ± 0.52	6.28 ± 0.99	5.02 ± 0.83	6.10 ± 1.20
	SAR		0.58 ± 0.25	0.32 ± 0.05	0.3 ± 0.12	2.83 ± 0.66
	EC	*dS/m*	0.14 ± 0.03	0.69 ± 0.09	0.14 ± 0.06	1.19 ± 0.29
	Calcium	*mg/kg*	4.05 ± 1.27	31.7 ± 9.42	4.68 ± 3.14	35.35 ± 12.62
	Magnesium	*mg/kg*	1.40 ± 0.46	8.38 ± 1.80	1.25 ± 0.80	11.18 ± 3.19
	Sodium	*mg/kg*	3.50 ± 1.73	4.75 ± 0.50	1.88 ± 1.55	46.75 ± 6.34
	Potassium	*mg/kg*	1.38 ± 0.75	2.00 ± 0.00	1.00 ± 0.71	3.75 ± 1.71
	Chloride	*mg/kg*	3.00 ± 0.82	3.75 ± 0.50	2.12 ± 2.02	8.75 ± 4.03
	Sulfate-SO_4	*mg/kg*	17.23 ± 5.62	111.72 ± 27.88	18.38 ± 12.85	210 ± 56.79
	Nitrate + Nitrite-N	*mg/kg*	1.25 ± 0.29	n.d.	1.12 ± 0.25	n.d.
Unplanted	pH		7.00 ± 0.72	8.10 ± 0.53	6.10 ± 1.87	7.28 ± 2.19
	SAR		0.33 ± 0.23	0.30 ± 0.10	0.20 ± 0.08	2.38 ± 0.32
	EC	*dS/m*	0.25 ± 0.03	0.37 ± 0.12	0.28 ± 0.21	0.97 ± 0.42
	Calcium	*mg/kg*	6.33 ± 1.14	19.03 ± 7.39	6.70 ± 2.50	27.70 ± 13.32
	Magnesium	*mg/kg*	1.87 ± 0.06	6.10 ± 1.73	2.05 ± 0.38	8.85 ± 2.97
	Sodium	*mg/kg*	2.33 ± 1.53	4.33 ± 0.58	1.75 ± 0.50	37.00 ± 3.65
	Potassium	*mg/kg*	5.00 ± 1.73	6.33 ± 3.21	3.00 ± 0.82	6.25 ± 1.26
	Chloride	*mg/kg*	4.33 ± 0.58	7.00 ± 3.61	3.25 ± 0.50	10.75 ± 2.63
	Sulfate-SO_4	*mg/kg*	27.57 ± 6.73	53.30 ± 28.14	27.45 ± 21.85	156.50 ± 64.48
	Nitrate + Nitrite-N	*mg/kg*	1.00 ± 0.00	n.d.	1.12 ± 0.25	n.d.

Water Chemistry

The GLM showed that both water type and plant treatment significantly influenced final water chemistry (Table S4). OSPW mesocosms had higher alkalinity, EC, TDS, hardness, and concentrations of Cl, K, Mg, Na, and SO_4 than RO mesocosms ($p<0.05$), consistent with the characteristic chemistry of untreated OSPW (elevated pH and salinity) (Mahaffey and Dubé 2017). Within OSPW treatments, unplanted mesocosms exhibited the highest EC, TDS, and SO_4, whereas *T. latifolia* reduced these values, suggesting uptake or retention effects. Plant species also differed in their influence, with water from *T. latifolia* mesocosms containing significantly lower K and Cl than *J. balticus* ($p<0.05$). Across both water types, planted mesocosms generally had higher alkalinity and Ca than unplanted controls, while unplanted mesocosms had the highest pH and conservative ion concentrations.

As expected, addition of untreated OSPW resulted in elevated salinity, with final SO_4 concentrations ranging from 304.8 to 438.8 mg/L. However, RO mesocosms also showed marked increases in Ca, Mg, SO_4, and alkalinity relative to starting conditions (Table 2), implicating CST as a major internal solute source. Increases of Ca, Mg, and alkalinity in soils (Table 1) and overlying water (Table 2) are consistent with mineral weathering, particularly carbonate dissolution, which releases Ca^{2+} and HCO_3^-, enhancing alkalinity and base cation concentrations. Similar to soil redox, water ORP values exceeded 100 mV and dissolved oxygen levels remained above 5 mg/L throughout the experiment, indicating oxidizing conditions. Planting further modified water chemistry: planted mesocosms exhibited higher alkalinity than unplanted ones, consistent with rhizosphere-driven carbonate dissolution and biological CO_2 cycling. Root activity, especially in *T. latifolia*, likely stimulated microbial oxidation and respiration, producing

Table 2 Chemical properties (mean ± standard deviation, $n = 4$) of oil sands process-affected water (OSPW) and reverse osmosis (RO) water at 0 d (Initial) and 89 d (Final). Initial samples were collected during the mesocosm acclimation period, when all mesocosms contained RO water prior to draining and refilling with OSPW. DO: dissolved oxygen; EC: electrical conductivity; TDS: total dissolved solids

	Parameter	Units	Initial	RO Final	OSPW Final
J.balticus	pH		6.35 ± 0.46	7.93 ± 0.61	7.80 ± 0.21
	EC	dS/m	0.08 ± 0.03	0.45 ± 0.08	1.15 ± 0.08
	TDS	mg/L	36.12 ± 12.68	261.00 ± 54.35	754.25 ± 62.67
	Alkalinity	mg/L as $CaCO_3$	5.94 ± 2.48	123.00 ± 40.29	221.00 ± 4.55
	Bicarbonate	mg/L	3.94 ± 4.07	150.00 ± 49.30	269.25 ± 5.38
	Hardness	mg/L as $CaCO_3$	17.99 ± 8.05	205.00 ± 53.11	255.25 ± 13.62
	Calcium	mg/L	4.64 ± 2.24	52.27 ± 17.96	61.23 ± 3.09
	Iron	mg/L	0.02 ± 0.02	0.006 ± 0.002	0.01 ± 0.01
	Magnesium	mg/L	1.56 ± 0.69	18.12 ± 2.41	24.85 ± 1.72
	Manganese	mg/L	0.02 ± 0.05	< 0.005	< 0.005
	Sodium	mg/L	2.98 ± 0.84	11.93 ± 1.61	149.50 ± 19.67
	Potassium	mg/L	4.16 ± 0.68	3.75 ± 1.73	12.47 ± 1.35
	Chloride	mg/L	4.97 ± 0.66	11.35 ± 1.66	29.52 ± 2.67
	Sulfate (SO_4)	mg/L	14.35 ± 10.54	89.62 ± 20.95	344.00 ± 44.32
	Nitrate-N	mg/L	1.11 ± 0.70	< 0.01	< 0.01
T.latifolia	pH		5.92 ± 0.52	7.59 ± 0.11	7.70 ± 0.12
	EC	dS/m	0.02 ± 0.00	0.47 ± 0.01	1.03 ± 0.12
	TDS	mg/L	9.12 ± 2.64	277.50 ± 13.77	671.00 ± 94.67
	Alkalinity	mg/L as $CaCO_3$	5.62 ± 3.60	155.25 ± 15.95	214.25 ± 3.77
	Bicarbonate	mg/L	3.81 ± 3.71	189.25 ± 19.74	261.50 ± 4.73
	Hardness	mg/L as $CaCO_3$	3.12 ± 1.36	232.25 ± 6.90	268.00 ± 10.61
	Calcium	mg/L	0.84 ± 0.30	62.02 ± 2.33	65.80 ± 1.65
	Iron	mg/L	0.01 ± 0.01	0.02 ± 0.01	0.02 ± 0.01
	Magnesium	mg/L	0.30 ± 0.14	18.77 ± 0.36	25.18 ± 1.69
	Manganese	mg/L	0.01 ± 0.007	< 0.005	< 0.005
	Sodium	mg/L	1.18 ± 0.31	7.52 ± 2.76	130.50 ± 26.75
	Potassium	mg/L	0.56 ± 0.38	< 0.40	1.55 ± 1.00
	Chloride	mg/L	0.89 ± 0.27	0.95 ± 0.42	14.70 ± 4.52
	Sulfate (SO_4)	mg/L	2.72 ± 1.37	94.75 ± 5.24	304.75 ± 62.52
	Nitrate-N	mg/L	< 0.01	< 0.01	0.006 ± 0.002
Unplanted	pH		5.24 ± 1.05	8.29 ± 0.39	8.27 ± 0.26
	EC	dS/m	0.16 ± 0.22	0.39 ± 0.04	1.26 ± 0.08
	TDS	mg/L	45.57 ± 39.94	227.67 ± 28.11	833.00 ± 61.42
	Alkalinity	mg/L as $CaCO_3$	2.50 ± 0.00	65.00 ± 4.58	146.75 ± 21.90
	Bicarbonate	mg/L	2.50 ± 0.00	79.00 ± 5.57	178.75 ± 26.59
	Hardness	mg/L as $CaCO_3$	17.86 ± 6.74	162.67 ± 21.22	226.50 ± 50.82
	Calcium	mg/L	4.79 ± 2.04	37.73 ± 7.42	45.05 ± 18.62
	Iron	mg/L	0.92 ± 2.42	0.03 ± 0.02	0.01 ± 0.01
	Magnesium	mg/L	1.46 ± 0.43	16.63 ± 0.76	27.68 ± 1.25
	Manganese	mg/L	0.12 ± 0.15	< 0.005	< 0.005
	Sodium	mg/L	2.61 ± 0.23	12.33 ± 0.35	184.00 ± 4.24
	Potassium	mg/L	4.11 ± 0.97	6.27 ± 0.84	14.28 ± 1.79
	Chloride	mg/L	5.01 ± 1.10	13.23 ± 1.42	35.00 ± 2.29
	Sulfate (SO_4)	mg/L	27.44 ± 39.46	102.33 ± 16.29	438.75 ± 55.46
	Nitrate-N	mg/L	1.41 ± 1.22	< 0.01	< 0.01

CO_2 and H^+ that promoted mobilization of Ca, Mg and SO_4 (Ma et al. 2022).

pH dynamics reflected both abiotic buffering and biological influences. Although untreated OSPW is more alkaline than RO, the final pH values did not differ significantly between OSPW and RO treatments (7.6–7.9), instead all mesocosms increased relative to initial conditions (5.2–6.3). The highest pH occurred in unplanted mesocosms (up to 8.3), likely due to algae photosynthesis removing CO_2 and raising pH despite the lower alkalinity (Zerveas et al. 2021). In contrast, planted mesocosms maintained lower pH but higher alkalinity, reflecting rhizosphere respiration and carbonate dissolution that enhanced buffering capacity and moderated pH change. Other mesocosm studies have also reported similar patterns, with planted treatments maintaining lower pH than unplanted controls (McAndrew et al. 2017).

Because NAs are weak carboxylic acids, their speciation and mobility in oil sands process-affected water are strongly controlled by pH and alkalinity. Under the alkaline conditions typical of OSPW (pH ~ 8), NAs occur primarily as dissociated carboxylate anions, increasing aqueous solubility and influencing sorption and microbial degradation pathways that govern attenuation (Scott et al., 2005).

Overall, mesocosm water chemistry was shaped by the combined effects of external inputs (OSPW additions), internal solute release from CST weathering, and plant- and microbe-mediated processes. Plants reduced salinity and specific ion concentrations in a species-dependent manner, while also enhancing carbonate dissolution and CO_2 cycling. The result was a dynamic system where substrate weathering supplied ions and buffering capacity, while vegetation regulated CO_2 fluxes and moderated pH dynamics.

Plant Response

T. latifolia showed high survival in both RO (94%) and OSPW (96%) treatments by 88 d. Despite this, most individuals (~60%) had a vigor rating of 2 out of 7 (1 = fully dead, 7 = fully healthy), and all showed stress symptoms including wilting, mottling, necrosis, and chlorosis. Decline in health and vigor is likely linked to aphid infestations rather than water treatment, with infestations more severe in one greenhouse but not associated with treatment type. Plant height did not differ significantly between RO and OSPW ($p = 0.262$) and there was no significant water treatment × day interaction ($p = 0.470$). However, height declined significantly over time ($p < 0.001$), from 158.4 ± 8.8 cm to 73.8 ± 18.6 cm in OSPW, and from 163.5 ± 5.7 cm to 69.8 ± 24.6 cm in RO (Fig. 1). This decline likely reflected aphid damage to the primary shoots, as dieback reduced maximum height and subsequent measurements captured shorter secondary regrowth. Aboveground biomass showed a similar pattern and did not differ significantly between treatments (99.9 ± 52.1 g in RO vs. 96.9 ± 38.4 g in OSPW; $p = 0.929$), indicating no effect of water type on total plant biomass.

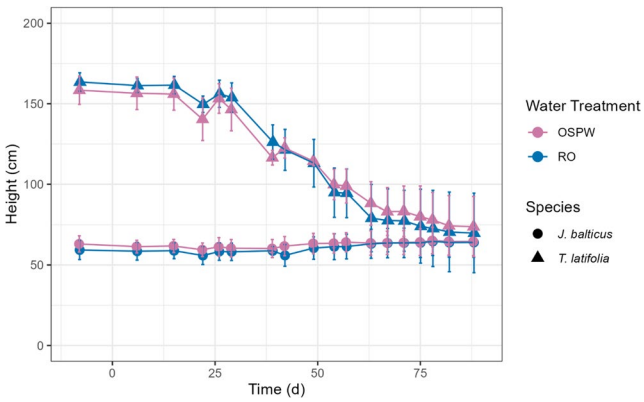


Fig. 1 Mean plant height and standard deviation for *J. balticus* and *T. latifolia* mesocosms in the oil sands process-affected water (OSPW) and reverse osmosis (RO) water treatments

J. balticus also showed similar survival, with 96% in RO water and 100% in OSPW treatments, and plants remained largely healthy and unaffected by the aphid outbreak. Most individuals (~60%) had vigor ratings of 4–6, indicating good condition, though some chlorosis, necrosis, and mottling were observed. The plants were actively growing, producing rhizomes, and a few plants flowered. Plant height was unaffected by water treatment ($p = 0.271$), day ($p = 0.545$), or their interaction ($p = 0.403$), remaining stable throughout the experiment. Heights increased slightly from 63.1 ± 5.0 cm prior to the experiment start during the pre-experiment acclimation phase, to 64.7 ± 8.8 cm at 88 d in OSPW, and from 59.4 ± 6.0 cm to 64.0 ± 9.3 cm in RO (Fig. 1). Aboveground biomass was similar between treatments (99.8 ± 46.6 g in RO vs. 86.5 ± 37.1 g in OSPW; $p = 0.672$), consistent with the stability of plant height and vigor.

Within the aboveground tissue, most measured parameters differed significantly between plant species but not between water types or by their interaction (Table S5, Fig S2). Multivariate analysis (PCA) confirmed these species-based differences, with clear separation between *J. balticus* and *T. latifolia* along PC1 (Fig S3). Overall, trace metal uptake (Fe, Mn, Zn, Cu) was linked to CST substrate, where concentrations were naturally high and variable, particularly for iron. This heterogeneity likely contributed to variability in plant tissue, with uptake patterns reflecting species-specific differences rather than water treatment.

J. balticus tissue accumulated higher concentrations of macronutrients (N, P, S) and several micronutrients/trace metals (Zn, Mg, Mn, Cu, Fe) compared to *T. latifolia* across both water types (Table 3, Fig S3). The greater concentrations observed in *J. balticus* likely reflect its overall better health conditions (active growth, no aphid infestation) during the experiment. By contrast, stress and dieback in *T. latifolia* may have reduced its growth and nutrient assimilation capacity. Accordingly, differences in tissue chemistry should be interpreted with consideration of differing stress rather than solely intrinsic uptake capacity. Despite its reduced vigor, *T. latifolia* tissue contained higher Ca and K, consistent with lower K concentrations in the water and soil of *T. latifolia* mesocosms (Tables 1 and 2). This aligns with previous reports that *T. latifolia* efficiently removes K (Geurts et al. 2020). Elevated Ca concentrations in water and soil are likely explained by ongoing mineral dissolution from CST, as discussed above.

Fe, Mn and Zn were the most abundant metals in the plant tissue. Despite high variability among replicates, Fe was consistently higher in *J. balticus* (265–725 µg/g) than

Table 3 *T. latifolia* and *J. balticus* tissue ion concentrations in reverse osmosis (RO) and oil sands process-affected water (OSPW) treatments after 89 d, expressed in mean ± standard deviation ($n = 4$)

	Tissue Ion	Units	RO Treatment	OSPW Treatment
J. balticus	Total Nitrogen	%	1.77 ± 0.21	1.74 ± 0.14
	Phosphorus	%	0.24 ± 0.03	0.22 ± 0.01
	Potassium	%	1.82 ± 0.24	1.95 ± 0.06
	Calcium	%	0.48 ± 0.02	0.36 ± 0.07
	Magnesium	%	0.27 ± 0.05	0.22 ± 0.02
	Sulfur	%	0.34 ± 0.05	0.38 ± 0.04
	Sodium	%	0.16 ± 0.05	0.49 ± 0.07
	Boron	µg/g	19.75 ± 10.44	30.25 ± 3.77
	Copper	µg/g	6.72 ± 2.91	6.00 ± 1.49
	Iron	µg/g	725.00 ± 756.02	265.00 ± 230.00
	Manganese	µg/g	210.00 ± 71.65	172.50 ± 26.30
	Molybdenum	µg/g	0.69 ± 0.34	1.25 ± 0.50
	Zinc	µg/g	57.00 ± 13.49	63.00 ± 4.24
T. latifolia	Total Nitrogen	%	1.04 ± 0.14	0.85 ± 0.13
	Phosphorus	%	0.14 ± 0.03	0.12 ± 0.03
	Potassium	%	2.12 ± 0.67	2.45 ± 0.35
	Calcium	%	0.72 ± 0.08	0.58 ± 0.06
	Magnesium	%	0.22 ± 0.02	0.17 ± 0.05
	Sulfur	%	0.14 ± 0.02	0.17 ± 0.04
	Sodium	%	0.44 ± 0.06	0.52 ± 0.07
	Boron	µg/g	19.75 ± 9.95	25.75 ± 9.46
	Copper	µg/g	5.25 ± 1.35	3.90 ± 0.64
	Iron	µg/g	76.00 ± 33.38	45.50 ± 17.90
	Manganese	µg/g	143.30 ± 44.60	96.0 ± 29.20
	Molybdenum	µg/g	0.55 ± 0.35	1.48 ± 0.61
	Zinc	µg/g	24.25 ± 5.32	18.50 ± 5.20

in *T. latifolia* (45–76 µg/g) (Table 3). Fe was also abundant in CST (~600–2700 mg/kg at 88 d; Table S2), and replicate variability in both CST and plant tissue likely reflects CST heterogeneity. On average, Fe in plant tissue and CST was higher in RO mesocosms than in OSPW mesocosms. Similarly, Mn and Zn were highest in *J. balticus* in RO treatments. Although Mn was below detection in CST and RO, its abundance in tissue suggests uptake from localized pools in CST (Tables 1 and 2). By contrast, Zn concentrations in CST (2.8–4.5 mg/kg; Table S2) were consistent across treatments, suggesting that interspecific differences reflect plant uptake capacity rather than substrate availability.

Plant tissue also showed elevated B, with slightly higher average concentrations in OSPW (25–30 µg/g) compared to RO (~19 µg/g), though differences were not statistically significant (Table S5). While B was not directly measured in OSPW, higher tissue concentrations under OSPW treatments and elevated B in CST in OSPW treatments (0.46–0.48 mg/kg) relatively to RO (0.18–0.28 mg/kg; Table S2) suggest a combined influence of water and substrate. The most definitive water-treatment effect was seen in Na (Table S5, Fig S2). OSPW contained considerably more Na than RO water (Table 2), which was reflected in significantly elevated Na in *J. balticus* under OSPW (0.46%) compared to RO water (0.16%). In contrast, *T. latifolia* exhibited similar tissue Na levels across water types (0.44–0.52%), suggesting species-specific Na regulation.

Naphthenic Acid Fraction Compound Dynamics

NAFC Composition and Molecular Characterization

NAFC concentrations declined across all OSPW treatments, starting at 50.3 ± 6.8 mg/L initially and by 89 d, final levels had decreased by 16% (42.3 ± 5.5 mg/L), 30% (35.3 ± 5.3 mg/L) and 40% (30.1 ± 7.1 mg/L), in unplanted, *J. balticus* and *T. latifolia* treatments, respectively (Fig. 2). By contrast, RO treatments gained negligible amounts of organic acidic material over time (i.e., within-error). NAFC reduction rates in mesocosms with OSPW ranged between 0.13 and 0.27 mg/L/d. These rates are within-range of a field-constructed wetland treatment system, representing 24 to 108% of NAFC reduction rates measured in the Kearl pilot-scale treatment wetland (Vander Meulen et al. 2025). Regardless, both *J. balticus* and *T. latifolia* treatments had NAFC reduction rates exceeding those of unplanted mesocosms, suggesting that these plants uptake, degrade, or otherwise support processes that reduce NAFC concentrations.

Previous mesocosm experiments have shown contrasting outcomes depending on plant species and substrate composition. *C. aquatilis* grown in mesocosms with a layered CST-peat substrate achieved substantially greater NAFC reductions than unplanted controls (Trepanier et al. 2023), whereas NAFC attenuation in *Scirpus microcarpus* and *Triglochin maritima* mesocosms with CST alone did not differ from unplanted treatments (Trepanier et al. 2025). The latter study suggested that the absence of a peat-based layer may have reduced nutrient availability and limited plant effects. In the present study, however, planted treatments enhanced NAFC removal despite the absence of peat, suggesting that factors beyond substrate nutrient supply can mediate plant effects. However, a low level of fertilization was applied in the present study during the pre-experiment acclimation phase to support plant establishment. Although most added nutrients were depleted the system was drained and flushed before the experiment began and most added nutrients were depleted, this early fertilization may have contributed to improved plant health at the start of the experiment and partly explain the difference in treatment response compared to the previous study. Plant species identity may also have been particularly important, as both *J. balticus* and *T. latifolia* promoted additional NAFC removal in the CST-only substrate. Notably, *T. latifolia* supported higher NAFC reductions despite reduced plant health. This suggests that NAFC attenuation in these systems may be influenced not

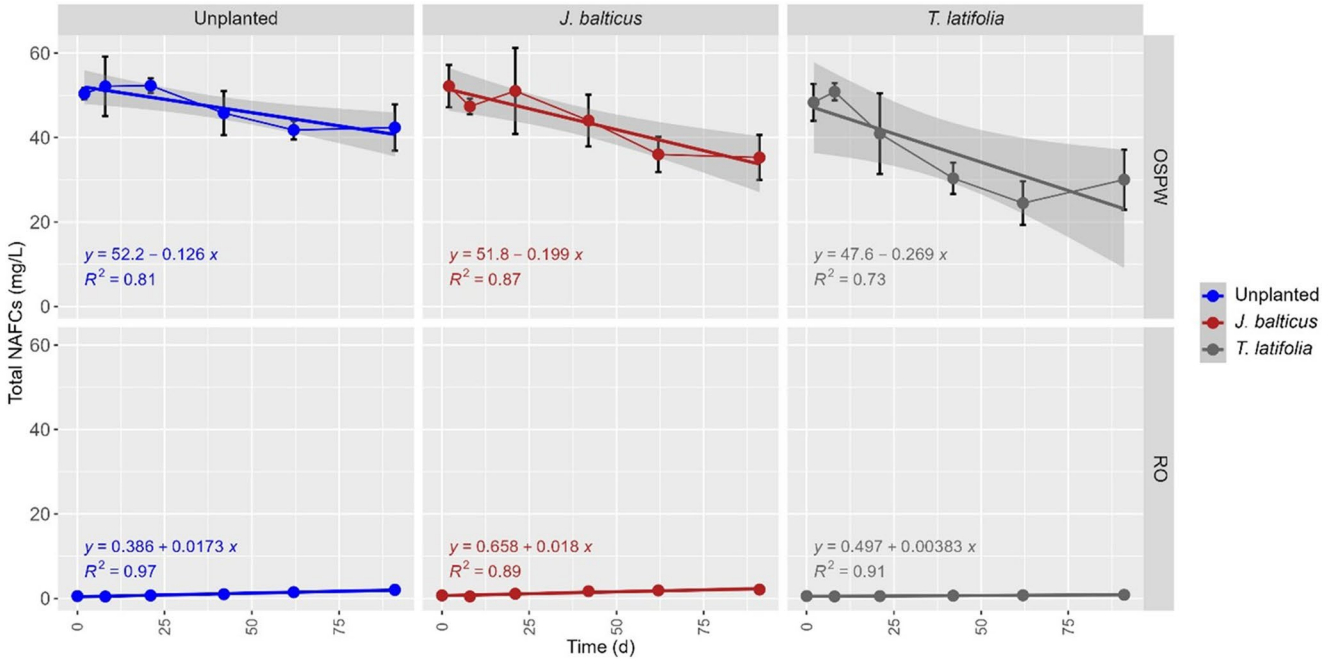


Fig. 2 Concentrations of total naphthenic acid fraction compounds (NAFCs) in all plant treatments (Unplanted, *J. balticus*, *T. latifolia*), water types (oil sands process-affected water (OSPW) and reverse osmosis (RO)), and sampling time points (0–89 d), where $n=4$ at each sampling event. Error bars represent ± 1 standard deviation on quantification

only by plant growth, but also by rhizosphere-mediated microbial processes that persist under plant stress. Potential mechanisms include the release of root exudates or labile organic carbon from root turnover and shoot dieback, which may stimulate heterotrophic microbial activity and co-metabolic degradation of NAFCs (Eze and Amuji 2024; Kalinowski and Halden 2012; Schultz et al. 2013). These putative plant-microbe interactions are explored further in the microbial analyses (Sect. 3.5).

With respect to compositional features of NAFCs detected by high-resolution analyses, the overall trend was oxidizing, shown in Fig. 3. In unplanted mesocosms, O_2-NAFCs (i.e., mostly classical NAs) decreased from ~55% to 33% mass spectral abundance (base-peak normalized abundance). In comparison, in mesocosms with *J. balticus* or *T. latifolia*, O_2-NAFCs decreased to 25% and 18% abundances, respectively. These correspond to average reduction rates of 0.24%/d, 0.33%/d, and 0.41%/d of O_2-NAFCs respectively for unplanted, *J. balticus*, and *T. latifolia* mesocosms. While reduction of O_2-NAFCs is here estimated as a simple linear relationship with time, the relationship has a practical limit, as O_2-NAFCs are never completely eliminated, even in exceptionally mature wetlands (Vander Meulen et al. 2021a, b). In these mesocosms, O_3- and O_4-NAFCs increased proportionally to decreases in O_2-NAFCs. Small abundances of O_2S-containing formulae were initially detected in all OSPW-containing mesocosms, but these were no longer observed past sampling by 6 d. Heteroatom trends in RO treatments were largely unremarkable with large relative error, suggesting that trends in the OSPW-containing treatments would be attributable to factors excluding direct mobilization of soil carbon. These changes might be anticipated to correspond to lesser overall toxicity of NAFCs in OSPW with treatments, as might naturally be expected from mitigating toxic O_2-NAFCs (Hughes et al. 2017).

To investigate relative compositional differences in these time-series samples, spectral data were ordinated by use of PCA, shown in Fig S4. The majority of variance in these treatments is explained along the first principal component (PC1; 78.8% explained variance), corresponding largely in-line with trends described by the prior figures. The mesocosms planted with *T. latifolia* showed the greatest end-to-end compositional difference over the treatment period, spanning the entirety of the PC1 axis. In comparison, between 1 d (after OSPW addition) and 89 d, *J. balticus* mesocosms reach a maximum PC1 coordinate of ~16, or approximately 30 units removed from the initial condition, indicating that degradation is still happening in these treatments. The unplanted treatments deviate less from their initial condition at 1 d, only reaching between PC1 coordinate 0–10 by 89 d. Thus, all treatments exhibited a similar overall chemical trajectory, where mesocosms with *T. latifolia* had the greatest overall compositional changes. The range of spectral outcomes is broad by 89 d, as is shown by the relative spread of sample coordinates along PC1 in Fig S4; this variability is also reflected in Fig. 3 as error bars on

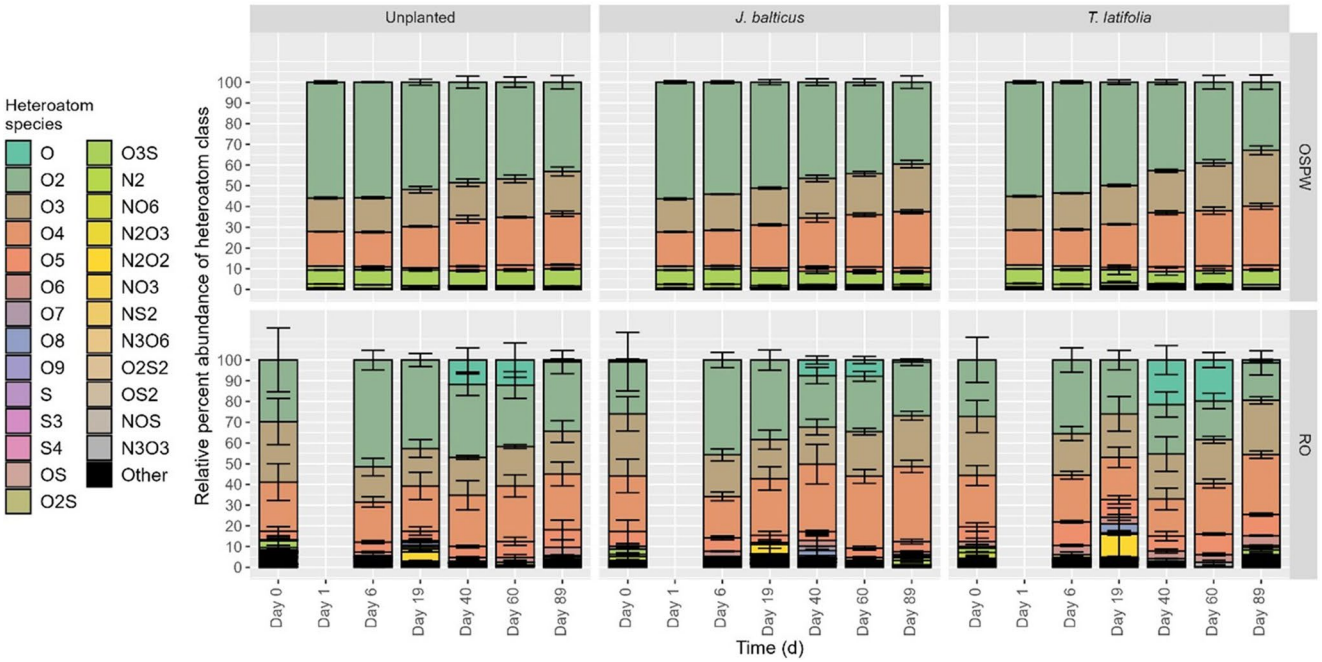


Fig. 3 Spectral compositions of all assigned naphthenic acid fraction compounds (NAFCs) in water samples from all plant treatments (Unplanted, *J. balticus*, *T. latifolia*), water types (oil sands process-affected water (OSPW) and reverse osmosis (RO)), and sampling time points, where $n=4$ at each sampling event. Day 0 represents mesocosms prior to OSPW addition. Error bars represent ± 1 standard deviation on quantification

assignments become broader over time, and could reflect the influence of impairments resulting from differential levels of aphid infestations, as was mentioned earlier. Nonetheless, both the total heteroatoms and PCA reflect a consistent trend in oxidation and degradation of NAFCs. However, high-resolution MS alone cannot distinguish between biodegradation, plant uptake, or sorption processes. Stable carbon isotope analysis (Sect. 3.4.2) provides an independent line of evidence for selective removal of bitumen-derived NAFCs.

NAFC Isotopic Signature

The average $\delta^{13}C_{pyr}$ values of NAFCs determined in OSPW samples ($n=3$ or 4) from Unplanted, *J. balticus* and *T. latifolia* mesocosms collected on 0 d (prior to addition of OSPW), 6 d, 19 d, 40 d, 60 d and 89 d are plotted on Fig. 4. The average $\delta^{13}C_{pyr}$ values in the two planted mesocosms (*J. balticus* and *T. latifolia*) on 0 d were -28.6 ± 0.9‰ and -29.0 ± 1.2‰, respectively, and were similar to those previously found for NAFCs originating from non-bitumen-derived plant/soil organic matter (Ahad et al. 2013, 2020; Gibson et al. 2025; Trepanier et al. 2025). The slightly heavier $\delta^{13}C_{pyr}$ value for the Unplanted treatment on 0 d (-25.1 ± 0.8‰) can be attributed to the lack of plant material and a background signal in CST likely containing residual bitumen-derived NAFCs having a $\delta^{13}C_{pyr}$ value of around −21‰ (Ahad et al. 2012, 2013, 2020; Gibson et al. 2025).

As illustrated on Fig. 4, the $\delta^{13}C_{pyr}$ values in all three treatments six days following the addition of OSPW were considerably more positive compared to the relatively ^{13}C-depleted background signals on 0 d, reflecting an isotopic shift towards that of the dominant source bitumen-derived

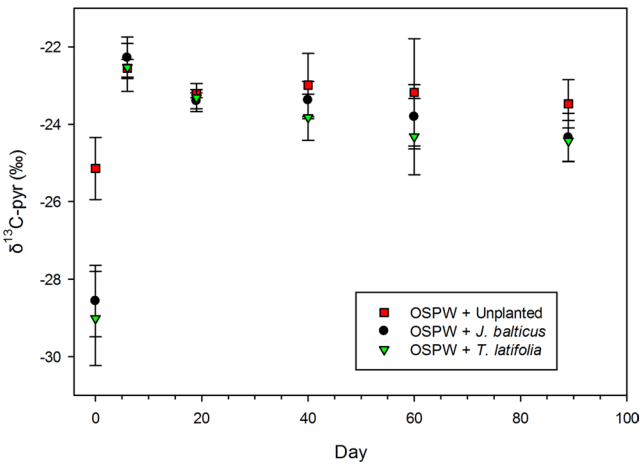


Fig. 4 $\delta^{13}C_{pyr}$ values of naphthenic acid fraction compounds (NAFCs) in all treatments (Unplanted, *J. balticus*, *T. latifolia*) for oil sands process-affected water (OSPW), and sampling time points (0–89 d), where $n=3$ or 4 at each sampling event. Day 0 represents mesocosms prior to OSPW addition. Error bars represent ± 1 standard deviation on quantification

NAFCs (~ −21‰). From 6 d to the last sampling point (89 d), $\delta^{13}C_{pyr}$ values in all three treatments showed a progressive decrease, ranging from −22.6‰, −22.3‰ and −22.5‰ to −23.5‰, −24.3‰ and −24.4‰ in Unplanted, *J. balticus* and *T. latifolia* treatments, respectively. After 40 d, Unplanted treatments began to deviate from planted treatments, showing slightly more positive values (between 0.6 to 0.9‰) compared to the combined average values for the planted mesocosms. Both Time ($p < 0.001$) and Treatment × Time ($p < 0.05$) showed a significant effect, with significant declines from 6 d to 89 d for each treatment ($p < 0.01$), and *T. latifolia* significantly more depleted ($p = 0.029$) and *J. balticus* marginally more depleted ($p = 0.051$) than Unplanted mesocosms at 89 d. There were no discernible differences in the overall trends found for both planted treatments.

Degradation of dissolved organic mater (DOM) is often associated with carbon isotope fractionation, whereby the residual DOM pool becomes progressively enriched in ^{13}C due to preferential breakdown of ^{12}C-containing bonds (Vähätalo and Wetzel 2008; Zheng et al. 2025). In contrast, $\delta^{13}C_{pyr}$ values in this study shifted toward more negative values despite decreases in NAFC concentrations (Fig. 2) and increases in the proportion of oxidized NAFC species (Fig. 3). Thus, rather than a classic isotope fractionation effect from the preferential breakdown of isotopically lighter components within the NAFC pool, attenuation resulted in the selective removal of isotopically heavier bitumen-derived NAFCs (~ −21‰), leaving behind a residual more closely reflecting the relatively ^{13}C-depleted background signal. A similar process of selective removal of isotopically heavier components leaving behind more negative $\delta^{13}C$ values has previously been inferred during early diagenesis in sediments (Böttcher et al. 1998; Liu et al. 2020).

The distinct temporal shift toward more negative $\delta^{13}C_{pyr}$ values observed in this study (Fig. 4) contrasts with the more stable isotopic signature reported by Trepanier et al. (2023) in unplanted and planted (*C. aquatilis*) mesocosms. In that study, $\delta^{13}C_{pyr}$ values ranged from −22.5 to −19.5‰ in unplanted and −21.8 to −20.9‰ in planted treatments, with the percent abundance of O_2–NAFCs remaining relatively high (~55–65%) over 84 days. The change in $\delta^{13}C_{pyr}$ and O_2–NAFCs composition was attributed primarily to sorption processes associated with the peat-based substrate used in that study, which provides substantial sorption capacity for NAFC retention. However, the slight decrease in $\delta^{13}C_{pyr}$ observed in the planted treatments suggests that some biotransformation may still have occurred, even in the presence peat-based substrate (Trepanier et al. 2023). In contrast, the CST substrate used in the present study contains little organic matter, minimizing sorption to the substrate and allowing isotopic shifts associated with OSPW-derived NAFC transformation to be more clearly expressed.

Another investigation examining OSPW attenuation using *S. microcarpus*, *T. maritima* and unplanted controls reported a similar range of relatively ^{13}C-depleted $\delta^{13}C_{pyr}$ values to those found here (Trepanier et al. 2025). However, in contrast to the current study, no clear progressive shift toward negative values was observed, with $\delta^{13}C_{pyr}$ values in most mesocosms showing little variation between from around −24 to −22‰ at 10 d to the end of the experiment (78 d). While the reasons for this discrepancy remain uncertain, it is possible that more pronounced attenuation occurring during the early stages of the previous study played a role in masking the temporal isotopic trend found in the current study. Another factor distinguishing the current study is the development of plant detritus, particularly in *T. latifolia* mesocosms due to plant dieback, which likely influenced microbial and geochemical conditions. Decomposition of detritus can release nutrients that stimulate heterotrophic activity, create localized low-O_2 microsites, and may provide some sorptive surfaces for NAFCs. Indeed, *T. latifolia* mesocosms had the lowest mean dissolved O_2 in the bulk water over the experiment duration (≈6.3 ppm, compared with ≈8.9 ppm in *J. balticus* and ≈11.9 ppm in Unplanted mesocosms) and showed the greatest NAFC removal.

Taken together, the isotopic and compositional datasets provide complementary evidence of preferential removal of bitumen-derived components in the planted mesocosms. Progressive declines in O_2-NAFCs and overall oxidation trends observed by high-resolution MS, coupled with the concurrent shift toward more negative $\delta^{13}C_{pyr}$ values, support selective attenuation of isotopically heavier, bitumen-derived components rather than simple dilution of the NAFC pool. While sorption to detrital organic matter may have contributed, particularly in *T. latifolia* mesocosms, the combined NAFC and isotopic patterns are consistent with transformation processes occurring within the mesocosms. Given the low organic matter content of the CST substrate and observed oxygen dynamics microbially mediated degradation was likely a significant contributor and could have been augmented by co-metabolism on detrital substrates. Future work should further evaluate the role of plant-associated processes, including direct plant uptake and transformation, for example through quantification of NAFC accumulation in plant tissues. Additionally, upcoming experiments will specifically address whether sorption of OSPW-derived NAFCs to organic matter has an influence on $\delta^{13}C_{pyr}$ values.

Root Microbial Community

Microbial Diversity Dynamics

The time-pooled analysis of alpha diversity showed distinct strategies of recruiting microbes for *T. latifolia* and *J. balticus* in response to OSPW exposure (Fig. 5a; Table S6). *J. balticus* roots showed no difference in Richness (species count) between OSPW and RO treatments (adj $p=0.62$), while *T. latifolia* differed significantly between the two water types (adj $p=0.04$), with OSPW exposure leading to a net increase in the mean number of OTUs. Moreover, between the two species, *T. latifolia* also supported a significantly higher mean Richness than *J. balticus* in the OSPW treatments (adj $p=0.0005$). The higher richness observed in *T. latifolia* indicates that it either recruits more species through rhizodeposition or retains more of its original community following exposure to OSPW (Bulgarelli et al., 2013).

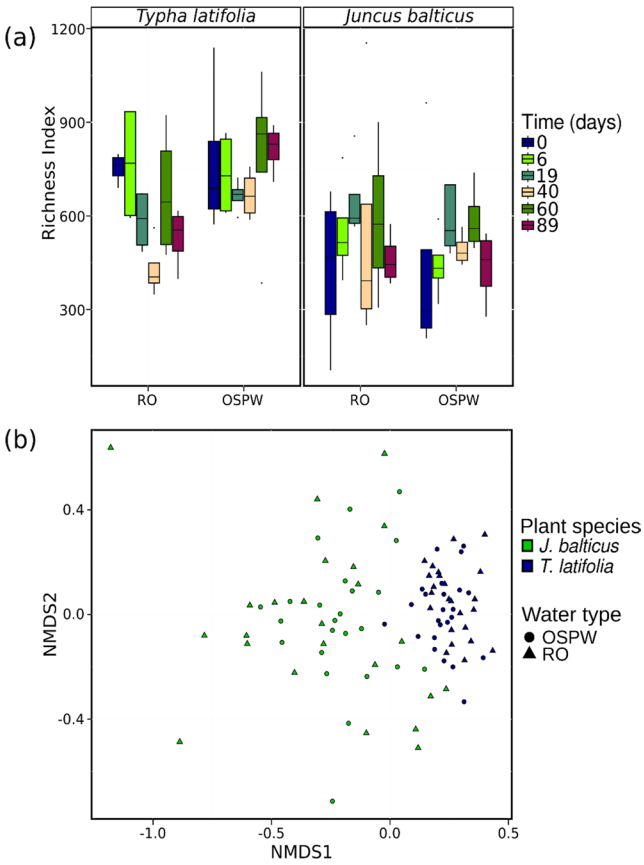


Fig. 5 Alpha and beta diversity of root-associated microbial communities in *T. latifolia* and *J. balticus* and across six time points (0 d to 89 d) under OSPW and RO treatments. (**a**) Alpha diversity was assessed using observed richness (OTU counts) and (**b**) beta diversity of microbial communities using NMDS based on Bray-Curtis distances. NMDS plots were colored by plant species and shaped by water type. 0 d represents samples collected before OSPW was added or RO was refilled

In contrast to richness, Shannon and Simpson indices (representing overall diversity and evenness) showed no significant difference between OSPW and RO treatments for either plant species, or between *T. latifolia* and *J. balticus* within the OSPW treatments (adj $p>0.05$) (Table S6). Therefore, the main distinction between *T. latifolia* and *J. balticus* was the total number of microbial species rather than the distribution of species within their communities. These microbial responses could be linked to the differences observed in NAFC attenuation, where *T. latifolia* demonstrated a higher capacity (~40% removal) compared to *J. balticus* (~30% removal).

Beta diversity was assessed using NMDS based on Bray-Curtis distances (Fig. 5b; Table S7). Results from PERMANOVA (differences in community composition) and PERMDISP (differences in variability) showed that OSPW effects were plant-specific and multidimensional, influencing both community structure and stability. In *T. latifolia*, microbial community composition was significantly altered by OSPW relative to RO water ($p=0.016$, $R^2 = 0.046$), aligning with the observed increase in microbial richness. PERMDISP indicated homogeneous dispersion ($p=0.53$), suggesting that *T. latifolia* drove a directed shift in community structure while maintaining stability. The higher capacity for NAFC removal observed in *T. latifolia* treatments corresponds with its higher microbial richness and compositional shift, indicating that microbial recruitment and restructuring enhanced NAFC degradation, as previously reported (Phillips et al. 2010). This stable, enriched community likely included specialized NAFC-degrading microorganisms promoted by root exudates (Chaparro et al. 2013), providing metabolic redundancy to sustain high removal rates despite reduced aboveground plant health.

In contrast, *J. balticus* exhibited a resistance strategy that compromised community stability. Its microbial composition did not shift significantly in response to OSPW (PERMANOVA: $p=0.25$, $R^2=0.025$). However, PERMDISP showed increased dispersion ($p=0.020$), indicating that OSPW affected community predictability and stability without driving a functional compositional change. This suggests that the *J. balticus* roots failed to recruit or enrich specialized NAFC degraders, resulting in random fluctuations among existing microbes (Allison and Martiny 2008). The absence of a directed, stable shift likely limited the establishment of robust catabolic pathways, contributing to lower NAFC removal compared to *T. latifolia*.

Comparing the two species within OSPW revealed that plant species was the dominant ecological filter driving a strong and highly significant difference in community composition (PERMANOVA, $p=0.001$, $R^2=0.20$), with dispersion also being significantly different (PERMDISP, $p=0.008$). Previous studies have shown that plant type can

influence and shift microbial communities over time, corresponding with NAFC removal – likely due to reduced toxicity from NAFC oxidation and increased nutrient availability resulting from plant stress in planted mesocosms (Trepanier et al. 2025).

UPGMA dendrograms (Bray-Curtis dissimilarity) further demonstrated clustering by plant species and water types (Fig S5). Samples from *T. latifolia* and *J. balticus* formed two major clades, reinforcing host selection as a dominant driver whereby plant-specific traits create distinct root niches that filter the background microbial pool (Byers et al. 2023). *T. latifolia* samples further grouped by time and treatment, with later stages (40 to 89 d) diverging from earlier samples, particularly under OSPW. *J. balticus* samples also clustered by water types and time, with the later OSPW-exposed roots (60 to 89 d) forming a tight cluster, suggesting stabilization under prolonged exposure. Roots exposed only to RO water showed a more variable trajectory, with 40 d samples forming a distinct subgroup. Overall, these results indicate that host identity is a key factor shaping microbial community, with water type and time also contributing to observed divergences, particularly in *J. balticus.*

Microbial Community Composition

Pseudomonadota consistently dominated root-associated bacterial communities across all time points in both species and water types (Fig. 6). In *J. balticus* roots, Pseudomonadota accounted for 58.4% at 0 d; following OSPW exposure after 6 d, their abundance rose to 65.9%, peaked at 79.7% by 19 d, and while still dominant, declined to 64.5%

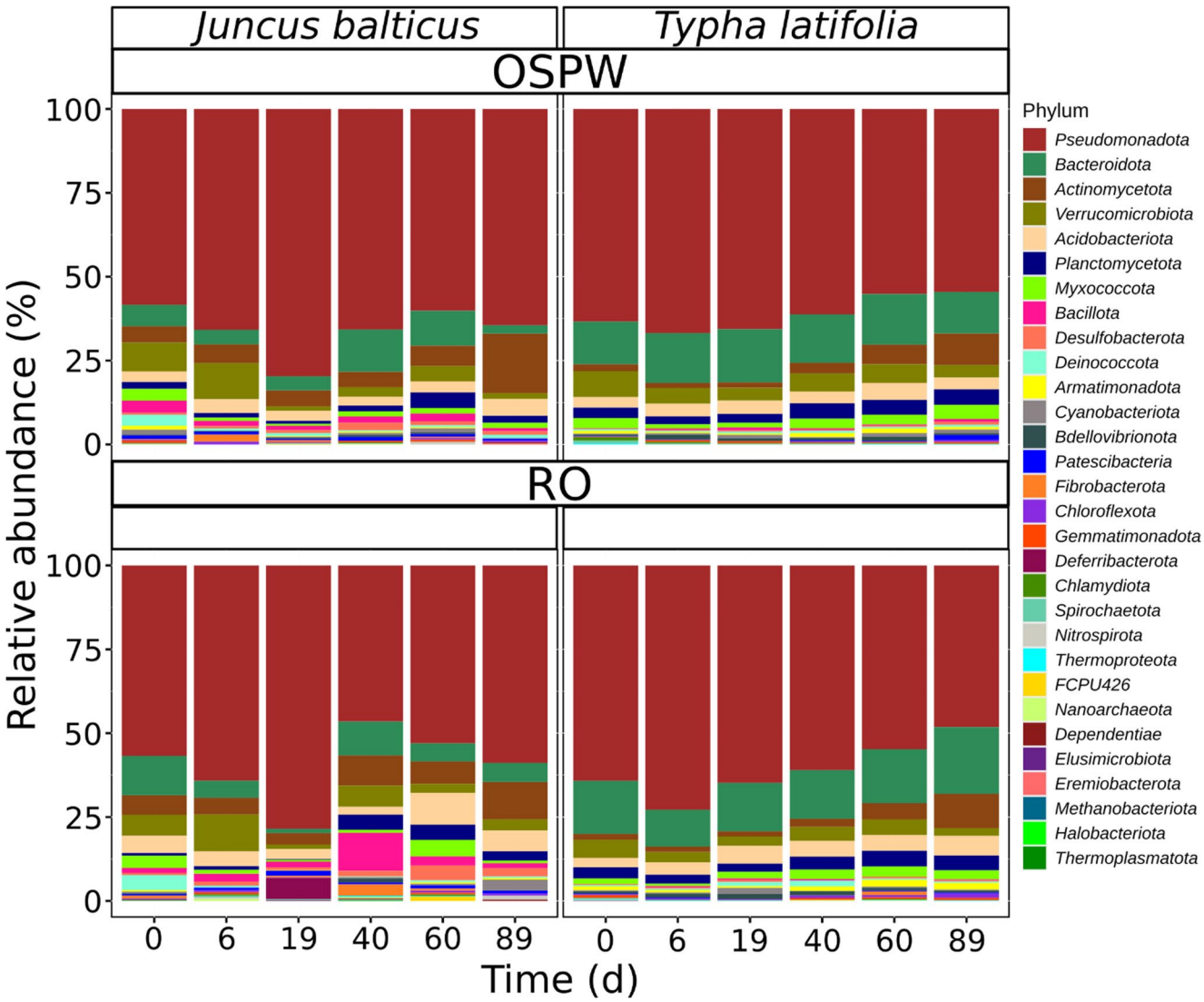


Fig. 6 Relative abundance of bacterial phyla across roots of plant species (*J. balticus* and *T. latifolia*), water types (OSPW and RO), and sampling time points (6 d, 19 d, 40 d, 60 d, 89 d). The 0 d represents samples collected before OSPW was added or RO was refilled

by 89 d. In *T. latifolia* roots, the abundance of Pseudomonadota similarly remained the most abundant phylum, rising slightly from 63.4% at 0 d to 66.8% after OSPW introduction at 6 d, before gradually declining to 54.5% 89 d. In RO treatments, Pseudomonadota also maintained dominance in both plant species, rising in *J. balticus* from 6 d (64.2%) to 19 d (78.5%) following the draining and refilling of RO at 6 d, before declining at 40 d (46.5%) and rising again by 89 d (58.9%). In *T. latifolia*, Pseudomonadota rose slightly at 6 d (72.8%) then declined steadily. This dominance is consistent with previous studies reporting Pseudomonadota enrichment in the rhizosphere and roots of *T. latifolia* (Faußer et al. 2012; Lagos et al. 2015; Li et al. 2013; Martínez-Martínez et al. 2023) and across wetland ecosystems (Liang et al. 2023; Zheng et al. 2024). Their prevalence in root systems is attributed to their capacity for rapid growth and broad metabolic versatility, particularly in utilizing diverse carbon substrates (Martínez-Martínez et al. 2023; Philippot et al. 2013).

The next most abundant phyla were Bacteroidota, Verrucomicrobiota, and Actinomycetota in both species and water types, with proportions varying over time. This community structure aligns with previous studies of root-associated microbiota dominated by Pseudomonadota, followed by these phyla (Lagos et al. 2015). Bacteroidota were particularly enriched in *T. latifolia* (up to 15.9%) and maintained consistently represented under both water types. This enrichment reflects *T. latifolia*'s relatively high root oxygen release, which can create localized micro-oxic rhizosphere zones that support aerobic and facultatively anaerobic bacteria even under generally low-oxygen conditions (Wießner et al. 2002). Actinomycetota increased at later time points (60–89 d), particularly in *J. balticus* (up to 17.8%), suggesting a successional pattern in root microbiome composition. Their enrichment may reflect their ability to degrade complex organic matter and tolerate nutrient-poor or oxygen limited environments, conferring a competitive advantage during later stages of rhizosphere colonization.

At the family-level, taxonomic composition varied with plant species, water type, and sampling time (Fig. 7). In *J. balticus* roots exposed to OSPW, *Gallionellaceae* consistently dominated, peaking at 19 d (49.5%) following OSPW exposure (28.8% at 6 d) before fluctuating thereafter, while *Burkholderiaceae* ranked second (6.0–13.0%). Families such as *Sphingomonadaceae*, *Xanthobacteraceae*, and *Opitutaceae* showed moderate but fluctuating levels. *Gallionellaceae* are chemolithoautotrophic iron oxidizers common in wetlands (Hallbeck and Pedersen 2014), where they contribute to root iron plaque formation and influence nutrient and metal uptake (Chan et al. 2023). Beyond iron oxidation, they also participate in organic matter degradation, plant colonization, immune interactions, nitrogen fixation and coupling Fe-S-P cycles (Chan et al. 2023; Hoover et al. 2023; Reis et al. 2014).

Under RO water, *J. balticus* roots exhibited a similar dominance of *Gallionellaceae*, peaking at 63.1% (19 d), with *Acidithiobacillaceae* and *Burkholderiaceae* being more abundant at 0 d and 40 d. *Acidithiobacillaceae* are active participants in Fe and S cycling (Rossoni et al. 2024) and contribute to organic hydrocarbon degradation (Xie et al. 2022). Overall, these functions likely contribute to the elevated Fe, S, and P concentrations observed in *J. balticus* tissues (Table 3). The heterogeneity of the CST bulk Fe suggests that iron-cycling at the root interface may influence metal partitioning and plant uptake in these mesocosms.

T. latifolia roots exposed to OSPW were primarily dominated by *Burkholderiaceae*, with a peak of 30.7% (6 d) and 27.0% (19 d), followed by *Chitinophagaceae*, *Xanthobacteraceae*, and *Sphingomonadaceae*. *Burkholderiaceae* are well established in rhizosphere environments and play key roles in degrading a range of organic pollutants, including toluene, naphthalene, benzene, and xylene (Kim et al. 2003; Lee et al. 2019; Lünsmann et al. 2016). The enrichment of hydrocarbon-degrading families in *T. latifolia* roots aligns with the greater NAFC declines observed in *T. latifolia* mesocosms and suggests that root-associated degraders, or rhizosphere conditions that favor them, may have contributed to NAFC attenuation. Other dominant families mentioned above are also recognized for their metabolic versatility in aromatic compound degradation, plant growth promotion, and bioremediation potential (Blanco-Enríquez et al. 2018; Ge et al. 2024; Li et al. 2021; Syranidou et al. 2018; Trepanier et al. 2025).

In addition, the substantial *T. latifolia* dieback observed in these mesocosms due to the aphid-infestation likely supplied labile detrital carbon that stimulated heterotrophic activity, as reflected in the lower dissolved oxygen levels (average ≈ 6.3 ppm) relative to other treatments. Microbial colonization of decaying detritus may have provided both nutrients and metabolic capacity for co-metabolism, whereby microbes using plant-derived carbon incidentally degrade hydrocarbons (Zhang et al. 2023). This interplay between root-associated degraders and detritus-driven microbial processes is consistent with the stronger NAFC removal observed in *T. latifolia* mesocosms. Dieback in *T. latifolia* therefore may have enhanced rhizosphere carbon availability and microbial recruitment, potentially increasing co-metabolic NAFC degradation despite reduced plant growth (Kalinowski and Halden 2012; Schultz et al. 2013). While this biotic stressor likely contributed to the treatment efficiency in *T. latifolia* mesocosms, it also introduces uncertainty when attributing differences in NAFC attenuation solely to intrinsic plant functional traits.

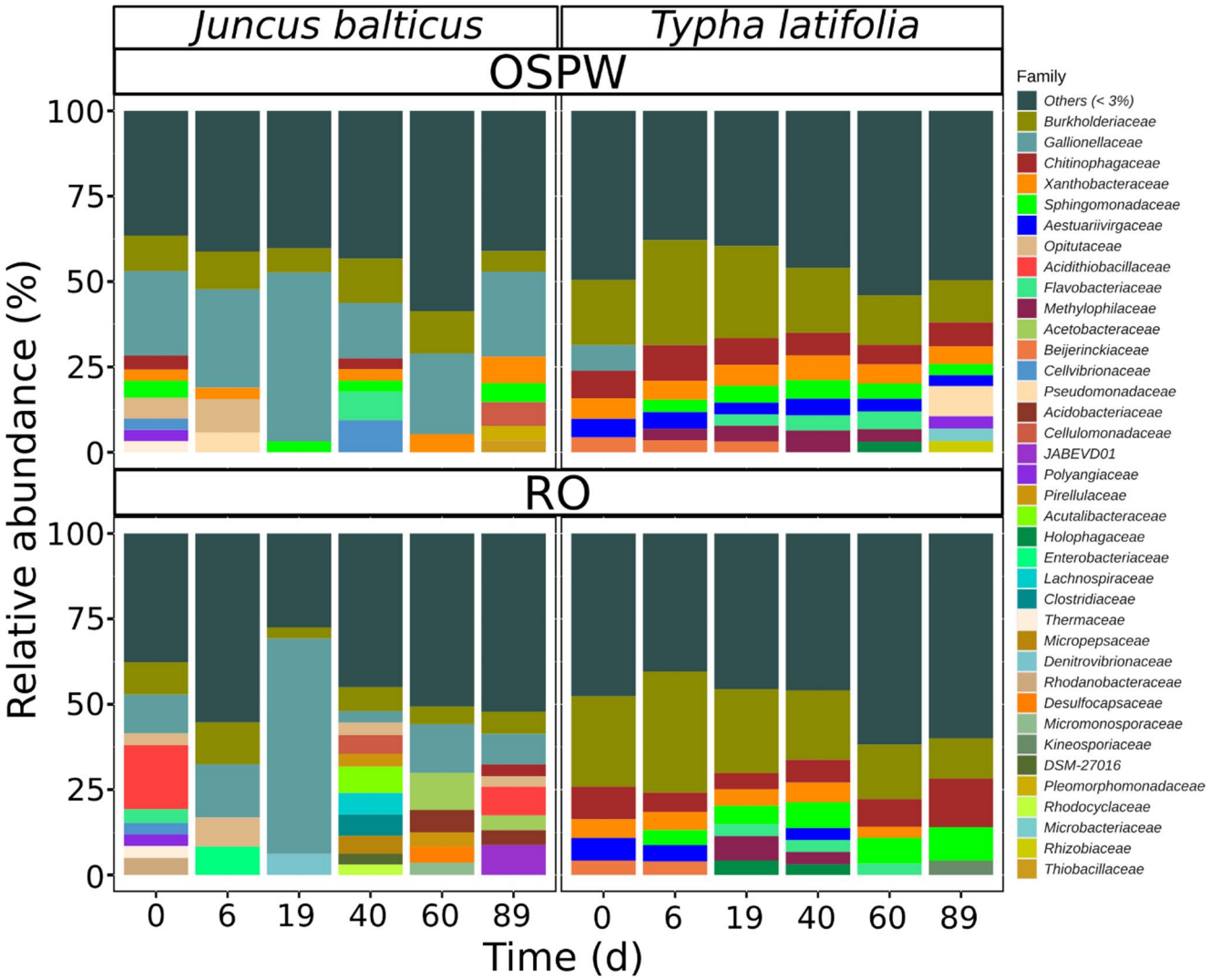


Fig. 7 Relative abundance of bacterial families across roots of plant species (*J. balticus* and *T. latifolia*), water types (OSPW and RO), and sampling time points (6 d,19 d, 40 d, 60 d, 89). The 0 d represents samples collected before OSPW was added or RO was refilled. Only families with relative abundance ≥ 3% in at least one sample are included

For *T. latifolia* under RO, *Burkholderiaceae* remained most abundant (35.4% at 6 d) before declining, while *Chitinophagaceae*, *Sphingomonadaceae*, *Methylophilaceae*, and *Aestuariivirgaceae* were more evenly distributed over time. *Methylophilaceae*, in particular, are known to degrade aromatic hydrocarbons (Lu et al. 2019). The detection of hydrocarbon-degrading taxa in roots of plants growing in RO water indicates that these groups are part of the resident root community. Many secondary metabolites from plants are structurally analogous to hydrocarbon contaminants (Singer et al. 2003), providing a mechanism by which these microbes are primed for degradation. Their presence implies that the root-associated community is functionally poised to degrade NAFCs when these compounds are introduced, highlighting the effectiveness of rhizoremediation strategies (Correa-García et al. 2018).

These family-level differences highlight the strong influence of plant species and water chemistry in shaping root microbiome structure. However, sediment DNA yields were insufficient for sequencing, and microbial analyses therefore focused exclusively on root samples. Root-associated communities are widely recognized as key for contaminant transformation in constructed wetland systems, as the root surfaces provide concentrated organic carbon inputs, oxygen gradients, and microbial attachment sites (Eze and Amuji 2024; Stottmeister et al. 2003). In the CST-based mesocosm system, which contained low organic matter, root-associated communities likely represented a dominant zone of microbial activity. Nevertheless, the absence of bulk substrate community data limits direct assessment of whole-system microbial partitioning in NAFC attenuation and the links observed here between the root microbiome composition

and NAFC removal should be interpreted as correlative. Future work should focus on optimizing the DNA extraction protocol for CST to improve the yields and allow for the characterization of their microbial communities.

Conclusion

This study identified plant-microbe-substrate interactions as potentially key mechanisms influencing CWTS performance and treatment outcomes. Plant species induced distinct shifts in water and soil chemistry, with changes in nutrient and ion concentrations (Ca, K, Mg, and SO_4) reflecting both uptake and plant-specific influences on substrate conditions. *T. latifolia* and *J. balticus* enhanced NAFC attenuation relative to unplanted controls, and while *J. balticus* maintained robust growth, *T. latifolia* achieved high NAFC removal even under reduced health, highlighting functional resilience. The composition of root microbial communities mirrored key chemical outcomes: *T. latifolia* supported a hydrocarbon degrader-rich microbiome associated with enhanced NAFC removal, whereas *J. balticus* hosted iron-cycling taxa that was linked to greater Fe uptake. By comparing OSPW and RO water, this study directly assessed how contaminant exposure shapes root microbiomes and whether plant species respond differently. *T. latifolia* showed increased richness and a directed compositional shift under OSPW, indicating targeted recruitment or restructuring of taxa, while *J. balticus* exhibited no compositional change but increased dispersion, reflecting a less predictable community that did not enrich specialized degraders. Although taxonomic data are correlative, they identify candidate functional groups for targeted functional validation and optimization of CWTS design. The presence of hydrocarbon degraders in RO systems further suggests latent microbial capacity that could be leveraged under contaminant stress. Overall, plant species appears to be an important contributor to remediation potential, underscoring the potential value of targeted plant selection in CWTS design for OSPW treatment.

Supplementary Information The online version contains supplementary material available at https://doi.org/10.1007/s13157-026-02074-3.

Acknowledgements We would like to thank Imperial Oil Ltd. for supporting this work and especially Dr. Carolina Berdugo-Clavijo for logistical and technical contributions. Special thanks to Kaitlyn Trepanier, Angie Van Dongen, Katelyn Grado, Jade Bergeron and Mouhcine Zentar for technical support. Funding support through a Genome Canada Large Scale Applied Research Project (LSARP) grant #18207 in partnership with Genome Alberta and Genome Quebec.

Author Contributions The manuscript was written through contributions of all authors. All authors have approved the final version of the manuscript. Amy-lynne Balaberda: Analysis; writing; and editing. Julius Eyiuche Nweze: Analysis; writing; and editing. Ian J. Vander Meulen: Sample processing; analysis; writing; and editing. Jason M. E. Ahad: Data analysis; writing; and editing. John V. Headley, Étienne Yergeau, and Christine Martineau: Experiment design; funding acquisition; writing and editing. Dani Degenhardt: Project management; experiment design; funding acquisition; writing and editing. All authors read and approved the final manuscript.

Funding Open access funding provided by Natural Resources Canada library. This work was support through a Genome Canada Large Scale Applied Research Project (LSARP) grant (#18207) in partnership with Genome Alberta and Genome Quebec.

Data Availability in your Statements & Declarations.
The datasets generated during and/or analysed during the current study are available from the corresponding author on reasonable request.

Declarations

Competing interests The authors have no relevant financial or non-financial interests to disclose.

Open Access This article is licensed under a Creative Commons Attribution 4.0 International License, which permits use, sharing, adaptation, distribution and reproduction in any medium or format, as long as you give appropriate credit to the original author(s) and the source, provide a link to the Creative Commons licence, and indicate if changes were made. The images or other third party material in this article are included in the article's Creative Commons licence, unless indicated otherwise in a credit line to the material. If material is not included in the article's Creative Commons licence and your intended use is not permitted by statutory regulation or exceeds the permitted use, you will need to obtain permission directly from the copyright holder. To view a copy of this licence, visit http://creativecommons.org/licenses/by/4.0/.

References

Abdalrhman AS, Zhang Y, Arslan M, Gamal El-Din M (2020) Low-current electro-oxidation enhanced the biodegradation of the recalcitrant naphthenic acids in oil sands process water. J Hazard Mater 398:122807. https://doi.org/10.1016/j.jhazmat.2020.122807

AEPA (2024a) Oil Sands Mine Water Science Team - Final technical reports and commentary. Alberta Environment and Protected Areas, Government of Alberta. https://open.alberta.ca/publications/oil-sands-mine-water-science-team-final-technical-reports-and-commentary

AEPA (2024b) Alberta Tier 1 soil and groundwater remediation guidelines (No. AEP, Land Policy, 2016, No. 3). Alberta Environment and Protected Areas (AEPA)

Ahad JME, Pakdel H, Gammon PR, Mayer B, Savard MM, Peru KM, Headley JV (2020) Distinguishing natural from anthropogenic sources of acid extractable organics in groundwater near Oil Sands tailings ponds. Environ Sci Technol 54:2790–2799. https://doi.org/10.1021/acs.est.9b06875

Ahad JME, Pakdel H, Gammon PR, Siddique T, Kuznetsova A, Savard MM (2018) Evaluating in situ biodegradation of 13 C-labelled naphthenic acids in groundwater near Oil Sands tailings ponds. Sci Total Environ 643:392–399. https://doi.org/10.1016/j.scitotenv.2018.06.159

Ahad JME, Pakdel H, Savard MM, Calderhead AI, Gammon PR, Rivera A, Peru KM, Headley JV (2013) Characterization and quantification of mining-related naphthenic acids in groundwater

near a major Oil Sands tailings pond. Environ Sci Technol 47:5023–5030. https://doi.org/10.1021/es3051313

Ahad JME, Pakdel H, Savard MM, Simard M-C, Smirnoff A (2012) Extraction, separation, and intramolecular carbon isotope characterization of Athabasca Oil Sands acids in environmental samples. Anal Chem 84:10419–10425. https://doi.org/10.1021/ac302680y

Ajaero C, Meulen IV, Simair MC, Le Roux M, Parrott J, Peru KM, McMartin DW, Headley JV (2020) Developments in molecular level characterization of naphthenic acid fraction compounds degradation in a constructed wetland treatment system. Environments 7:89. https://doi.org/10.3390/environments7100089

Ajaero C, Peru KM, Simair M, Friesen V, O'Sullivan G, Hughes SA, McMartin DW, Headley JV (2018) Fate and behavior of Oil Sands naphthenic acids in a pilot-scale treatment wetland as characterized by negative-ion electrospray ionization Orbitrap mass spectrometry. Sci Total Environ 631–632:829–839. https://doi.org/10.1016/j.scitotenv.2018.03.079

Alberta Energy Regulator (2024) State of Fluid Tailings Management for Mineable Oil Sands, 2023. Alberta Energy Regulator, Calgary, Alberta

Alberts ME, Wong J, Hindle R, Degenhardt D, Krygier R, Turner RJ, Muench DG (2021) Detection of naphthenic acid uptake into root and shoot tissues indicates a direct role for plants in the remediation of Oil Sands process-affected water. Sci Total Environ 795:148857. https://doi.org/10.1016/j.scitotenv.2021.148857

Allison SD, Martiny JBH (2008) Resistance, resilience, and redundancy in microbial communities. Proc Natl Acad Sci U S A 105:11512–11519. https://doi.org/10.1073/pnas.0801925105

Armstrong SA, Headley JV, Peru KM, Mikula RJ, Germida JJ (2010) Phytotoxicity and naphthenic acid dissipation from oil sands fine tailings treatments planted with the emergent macrophyte *Phragmites australis*. J Environ Sci Health A 45:1008–1016. https://doi.org/10.1080/10934521003772436

Balaberda A, Trepanier KE, Degenhardt D (2025) Mesocosm-Scale Constructed Wetland Design for Wastewater Treatment. JoVE 68195. https://doi.org/10.3791/68195

Blanco-Enríquez EG, Zavala-Díaz De La Serna FJ, Peralta-Pérez MDR, Ballinas-Casarrubias L, Salmerón I, Rubio-Arias H, Rocha-Gutiérrez BA (2018) Characterization of a microbial consortium for the bioremoval of polycyclic aromatic hydrocarbons (PAHs) in water. Int J Environ Res Public Health 15:975. https://doi.org/10.3390/ijerph15050975

Bolker BM, Brooks ME, Clark CJ, Geange SW, Poulsen JR, Stevens MHH, White JSS (2009) Generalized linear mixed models: a practical guide for ecology and evolution. Trends Ecol Evol 24:127–135. https://doi.org/10.1016/j.tree.2008.10.008

Böttcher ME, Oelschläger B, Höpner T, Brumsack H-J, Rullkötter J (1998) Sulfate reduction related to the early diagenetic degradation of organic matter and black spot formation in tidal sandflats of the German Wadden Sea (southern North Sea): stable isotope (13 C, 34S, 18O) and other geochemical results. Org Geochem 29:1517–1530. https://doi.org/10.1016/S0146-6380(98)00124-7

Brient JA, Wessner PJ, Merichem Company (2004) Naphthenic Acids. Kirk-Othermer Encyclopedia of Chemical Technology. Wiley Blackwell, United States, pp 509–514

Bulgarelli D, Schlaeppi K, Spaepen S, Van Themaat EVL, Schulze-Lefert P (2013) Structure and functions of the bacterial microbiota of plants. Annu Rev Plant Biol 64:807–838. https://doi.org/10.1146/annurev-arplant-050312-120106

Byers A-K, Condron LM, O'Callaghan M, Waller L, Dickie IA, Wakelin SA (2023) Plant species identity and plant-induced changes in soil physicochemistry—but not plant phylogeny or functional traits - shape the assembly of the root-associated soil microbiome. FEMS Microbiol Ecol 99:fiad126. https://doi.org/10.1093/femsec/fiad126

Cancelli AM, Gobas FAPC (2022) Treatment of naphthenic acids in oil sands process-affected waters with a surface flow treatment wetland: mass removal, half-life, and toxicity-reduction. Environ Res 213:113755. https://doi.org/10.1016/j.envres.2022.113755

Cancelli AM, Gobas FAPC (2024) Development and testing of a mechanistic model for wetland treatment of neutral and polar organic contaminants in oil sands process-affected water. Ecological Engineering 198:107145. https://doi.org/10.1016/j.ecoleng.2023.107145

Challis JK, Parajas A, Anderson JC et al (2020) Photodegradation of bitumen-derived organics in oil sands process-affected water. Environ Science: Processes Impacts 22:1243–1255. https://doi.org/10.1039/D0EM00005A

Chan CS, Dykes GE, Hoover RL, Limmer MA, Seyfferth AL (2023) Gallionellaceae in rice root plaque: metabolic roles in iron oxidation, nutrient cycling, and plant interactions. Appl Environ Microbiol 89:e00570-23. https://doi.org/10.1128/aem.00570-23

Chaparro JM, Badri DV, Bakker MG, Sugiyama A, Manter DK, Vivanco JM (2013) Root exudation of phytochemicals in *Arabidopsis* follows specific patterns that are developmentally programmed and correlate with soil microbial functions. PLoS ONE 8:e55731. https://doi.org/10.1371/journal.pone.0055731

Correa-García S, Pande P, Séguin A, St-Arnaud M, Yergeau E (2018) Rhizoremediation of petroleum hydrocarbons: a model system for plant microbiome manipulation. Microbial Biotechnology 11:819–832. https://doi.org/10.1111/1751-7915.13303

Eze MO, Amuji CF (2024) Elucidating the significant roles of root exudates in organic pollutant biotransformation within the rhizosphere. Sci Rep 14:2359. https://doi.org/10.1038/s41598-024-53027-x

Faulkner SP, Patrick WH, Gambrell RP (1989) Field techniques for measuring wetland soil parameters. Soil Sci Soc Amer J 53:883–890. https://doi.org/10.2136/sssaj1989.03615995005300030042x

Faußer AC, Hoppert M, Walther P, Kazda M (2012) Roots of the wetland plants *Typha latifolia* and *Phragmites australis* are inhabited by methanotrophic bacteria in biofilms. Flora - Morphology Distribution Funct Ecol Plants 207:775–782. https://doi.org/10.1016/j.flora.2012.09.002

Fox J, Weisberg S (2019) An R Companion to Applied Regression., Third Edition. ed. Sage, Thousand Oaks CA

Frank RA, Fischer K, Kavanagh R, Burnison BK, Arsenault G, Headley JV, Peru KM, Kraak GVD, Solomon KR (2009) Effect of carboxylic acid content on the acute toxicity of oil sands naphthenic acids. Environ Sci Technol 43:266–271. https://doi.org/10.1021/es8021057

Ge H, Liu X, Lu D, Yang Z, Li H (2024) Degradation of pyrene by *Xanthobacteraceae* bacterium strain S3 isolated from the rhizosphere sediment of *Vallisneria natans*: active conditions, metabolite identification, and proposed pathways. Environ Sci Pollut Res 31:25659–25670. https://doi.org/10.1007/s11356-024-32724-0

Geurts JJM, Oehmke C, Lambertini C, Eller F, Sorrell BK, Mandiola SR, Grootjans AP, Brix H, Wichtmann W, Lamers LPM, Fritz C (2020) Nutrient removal potential and biomass production by *Phragmites australis* and *Typha latifolia* on European rewetted peat and mineral soils. Sci Total Environ 747:141102. https://doi.org/10.1016/j.scitotenv.2020.141102

Gibson JJ, Jaggi A, Eby P, Sirbu T (2025) Stable isotope method for tracing oil sands bitumen sources, differentiating δ13C in four carbon fractions in water and acid-extractable organics. Sci Total Environ 998:180146. https://doi.org/10.1016/j.scitotenv.2025.180146

Gurney KE, Williams TD, Smits JE, Wayland M, Trudeau S, Bendell-Young LI (2005) Impact of oil-sands based wetlands on the growth of Mallard (*Anas platyrhynchos*) ducklings. Environ Toxicol Chem 24:457–463. https://doi.org/10.1897/03-575.1

Hallbeck L, Pedersen K (2014) The Family Gallionellaceae. In: Rosenberg E, DeLong EF, Lory S, Stackebrandt E, Thompson F (eds)

The Prokaryotes. Springer Berlin Heidelberg, Berlin, Heidelberg, pp 853–858. https://doi.org/10.1007/978-3-642-30197-1_398

Hanneseth AD, Brandal Ø, Sjöblom J (2006) Formation, growth, and inhibition of calcium naphthenate particles in oil/water systems as monitored by means of near infrared spectroscopy. J Dispers Sci Technol 27:185–192. https://doi.org/10.1080/01932690500265896

Harting F (2024) DHARMa: Residual Diagnostics for Hierarchical (Multi-Level / Mixed) Regression Models. R package version 0.4.7, CRAN. https://CRAN.R-project.org/package=DHARMa

Headley JV, Barrow MP, Peru KM, Fahlman B, Frank RA, Bickerton G, McMaster ME, Parrott J, Hewitt LM (2011) Preliminary fingerprinting of Athabasca oil sands polar organics in environmental samples using electrospray ionization Fourier transform ion cyclotron resonance mass spectrometry: FTICRMS fingerprinting of oil sands acids in environmental samples. Rapid Commun Mass Spectrom 25:1899–1909. https://doi.org/10.1002/rcm.5062

Headley JV, Peru KM, Fahlman B, Colodey A, McMartin DW (2013) Selective solvent extraction and characterization of the acid extractable fraction of Athabasca oils sands process waters by Orbitrap mass spectrometry. Int J Mass Spectrom 345–347:104–108. https://doi.org/10.1016/j.ijms.2012.08.023

Headley JV, Peru KM, McMartin DW, Winkler M (2002) Determination of dissolved naphthenic acids in natural waters by using negative-ion electrospray mass spectrometry. J AOAC Int 85:182–187. https://doi.org/10.1093/jaoac/85.1.182

Hendrikse M, Gaspari DP, McQueen AD, Kinley CM, Calomeni AJ, Geer TD, Simair MC, Peru KM, Headley JV, Rodgers JH, Castle JW (2018) Treatment of oil sands process-affected waters using a pilot-scale hybrid constructed wetland. Ecol Eng 115:45–57. https://doi.org/10.1016/j.ecoleng.2018.02.009

Hindle R, Headley J, Muench DG (2023) Pros and cons of separation, fractionation and cleanup for enhancement of the quantitative analysis of bitumen-derived organics in process-affected waters—a review. Separations Basel 10:583. https://doi.org/10.3390/separations10120583

Hoover RL, Keffer JL, Polson SW, Chan CS (2023) Gallionellaceae pangenomic analysis reveals insight into phylogeny, metabolic flexibility, and iron oxidation mechanisms. mSystems 8:e00038-23. https://doi.org/10.1128/msystems.00038-23

Huddleston GM, Rodgers JH (2008) Design of a constructed wetland system for treatment of copper-contaminated wastewater. Environ Geosci 15:9–19. https://doi.org/10.1306/eg.07250707006

Hughes SA, Mahaffey A, Shore B, Baker J, Kilgour B, Brown C, Peru KM, Headley JV, Bailey HC (2017) Using ultrahigh-resolution mass spectrometry and toxicity identification techniques to characterize the toxicity of oil sands process-affected water: the case for classical naphthenic acids: TIE of OSPW. Environ Toxicol Chem 36:3148–3157. https://doi.org/10.1002/etc.3892

Hussain NAS, Stafford JL (2023) Abiotic and biotic constituents of oil sands process-affected waters. J Environ Sci 127:169–186. https://doi.org/10.1016/j.jes.2022.06.012

Ivosev G, Burton L, Bonner R (2008) Dimensionality reduction and visualization in principal component analysis. Anal Chem 80:4933–4944. https://doi.org/10.1021/ac800110w

Janfada A, Headley JV, Peru KM, Barbour SL (2006) A laboratory evaluation of the sorption of oil sands naphthenic acids on organic rich soils. J Environ Sci Health Part A 41:985–997. https://doi.org/10.1080/10934520600620105

Kalinowski T, Halden RU (2012) Can stress enhance phytoremediation of polychlorinated biphenyls? Environ Eng Sci 29:1047–1052. https://doi.org/10.1089/ees.2012.0089

Kannel PR, Gan TY (2012) Naphthenic acids degradation and toxicity mitigation in tailings wastewater systems and aquatic environments: A review. J Environ Sci Health Part A 47:1–21. https://doi.org/10.1080/10934529.2012.629574

Kavanagh RJ, Frank RA, Burnison BK, Young RF, Fedorak PM, Solomon KR, Van Der Kraak G (2012) Fathead minnow (*Pimephales promelas*) reproduction is impaired when exposed to a naphthenic acid extract. Aquatic Toxicology 116–117:34–42. https://doi.org/10.1016/j.aquatox.2012.03.002

Khan S, Afzal M, Iqbal S, Khan QM (2013) Plant–bacteria partnerships for the remediation of hydrocarbon contaminated soils. Chemosphere 90:1317–1332. https://doi.org/10.1016/j.chemosphere.2012.09.045

Kim TJ, Lee EY, Kim YJ, Cho K-S, Ryu HW (2003) Degradation of polyaromatic hydrocarbons by *Burkholderia cepacia* 2A-12. World J Microbiol Biotechnol 19:411–417. https://doi.org/10.1023/A:1023998719787

Lagos L, Maruyama F, Nannipieri P, Mora ML, Ogram A, Jorquera MA (2015) Current overview on the study of bacteria in the rhizosphere by modern molecular techniques: a minireview. J Soil Sci Plant Nutr 0–0. https://doi.org/10.4067/S0718-95162015005000042

Lari E, Wiseman S, Mohaddes E, Morandi G, Alharbi H, Pyle GG (2016) Determining the effect of oil sands process-affected water on grazing behaviour of *Daphnia magna*, long-term consequences, and mechanism. Chemosphere 146:362–370. https://doi.org/10.1016/j.chemosphere.2015.12.037

Lee Y, Lee Y, Jeon CO (2019) Biodegradation of naphthalene, BTEX, and aliphatic hydrocarbons by *Paraburkholderia aromaticivorans* BN5 isolated from petroleum-contaminated soil. Sci Rep 9:860. https://doi.org/10.1038/s41598-018-36165-x

Lenth R, Piaskowski J, Banfai B, Bolker B, Buerkner P, Gine-Vazquez I, Herve M, Jung M, Love J, Miguez F, Riebl H, Singmann H (2025) emmeans: Estimated Marginal Means, aka Least-Squares Means. R package version 2 0 0. https://cran.r-project.org/web/packages/emmeans

Leshuk TMC, Young ZW, Wilson B, Chen ZQ, Smith DA, Lazaris G, Gopanchuk M, McLay S, Seelemann CA, Paradis T, Bekele A, Guest R, Massara H, White T, Zubot W, Letinski DJ, Redman AD, Allen DG, Gu F (2024) A Light Touch: Solar Photocatalysis Detoxifies Oil Sands Process-Affected Waters Prior to Significant Treatment of Naphthenic Acids. ACS EST Water acsestwater.3c00616. https://doi.org/10.1021/acsestwater.3c00616

Li C, Fu L, Stafford J, Belosevic M, Gamal El-Din M (2017) The toxicity of oil sands process-affected water (OSPW): A critical review. Science of The Total Environment 601–602:1785–1802. https://doi.org/10.1016/j.scitotenv.2017.06.024

Li Q, Li J, Jiang L, Sun Y, Luo C, Zhang G (2021) Diversity and structure of phenanthrene degrading bacterial communities associated with fungal bioremediation in petroleum contaminated soil. J Hazard Mater 403:123895. https://doi.org/10.1016/j.jhazmat.2020.123895

Li YH, Zhu JN, Liu QF, Liu Y, Liu M, Liu L, Zhang Q (2013) Comparison of the diversity of root-associated bacteria in *Phragmites australis* and *Typha angustifolia* L. in artificial wetlands. World J Microbiol Biotechnol 29:1499–1508. https://doi.org/10.1007/s11274-013-1316-2

Liang S, Li H, Wu H, Yan B, Song A (2023) Microorganisms in coastal wetland sediments: a review on microbial community structure, functional gene, and environmental potential. Front Microbiol 14:1163896. https://doi.org/10.3389/fmicb.2023.1163896

Lipnick R (1993) Baseline Toxicity QSAR Models: A Means to Assess Mechanism of Toxicity for Aquatic Organisms and Mammals, in: Gorsuch, J., Dwyer, F., Ingersoll, C., La Point, T. (Eds.), Environmental Toxicology and Risk Assessment: Second Volume. ASTM International, p. 0. https://doi.org/10.1520/STP13180S

Liu X, Hilfert L, Barth JAC, Van Geldem R, Friese K (2020) Isotope alteration caused by changes in biochemical composition of

sedimentary organic matter. Biogeochemistry 147:277–292. https://doi.org/10.1007/s10533-020-00640-3

Lu C, Hong Y, Liu J, Gao Y, Ma Z, Yang B, Ling W, Waigi MG (2019) A PAH-degrading bacterial community enriched with contaminated agricultural soil and its utility for microbial bioremediation. Environ Pollut 251:773–782. https://doi.org/10.1016/j.envpol.2019.05.044

Lünsmann V, Kappelmeyer U, Benndorf R, Martinez-Lavanchy PM, Taubert A, Adrian L, Duarte M, Pieper DH, Von Bergen M, Müller JA, Heipieper HJ, Jehmlich N (2016) In situ<Emphasis Type="SmallCaps">p</Emphasis> rotein- <Emphasis Type="SmallCaps">SIP</Emphasis> highlights Burkholderiaceae as key players degrading toluene by para ring hydroxylation in a constructed wetland model. Environ Microbiol 18:1176–1186. https://doi.org/10.1111/1462-2920.13133

Ma W, Tang S, Dengzeng Z, Zhang D, Zhang T, Ma X (2022) Root exudates contribute to belowground ecosystem hotspots: a review. Front Microbiol 13:937940. https://doi.org/10.3389/fmicb.2022.937940

Mahaffey A, Dubé M (2017) Review of the composition and toxicity of oil sands process-affected water. Environ Rev 25:97–114. https://doi.org/10.1139/er-2015-0060

Marentette JR, Frank RA, Bartlett AJ, Gillis PL, Hewitt LM, Peru KM, Headley JV, Brunswick P, Shang D, Parrott JL (2015) Toxicity of naphthenic acid fraction components extracted from fresh and aged oil sands process-affected waters, and commercial naphthenic acid mixtures, to fathead minnow (*Pimephales promelas*) embryos. Aquat Toxicol 164:108–117. https://doi.org/10.1016/j.aquatox.2015.04.024

Martínez-Martínez JG, Rosales-Loredo S, Hernández-Morales A, Arvizu-Gómez JL, Carranza-Álvarez C, Macías-Pérez JR, Rolón-Cárdenas GA, Pacheco-Aguilar JR (2023) Bacterial communities associated with the roots of *Typha* spp. and its relationship in phytoremediation processes. Microorganisms 11:1587. https://doi.org/10.3390/microorganisms11061587

Masliyah J, Zhou ZJ, Xu Z, Czarnecki J, Hamza H (2008) Understanding water-based bitumen extraction from Athabasca Oil Sands. Can J Chem Eng 82:628–654. https://doi.org/10.1002/cjce.5450820403

McAndrew B, Ahn C, Brooks J (2017) Effects of herbaceous planting richness on water physicochemistry in created mesocosm wetlands. J Freshw Ecol 32:119–132. https://doi.org/10.1080/02705060.2016.1248504

McKenzie N, Yue S, Liu X, Ramsay BA, Ramsay JA (2014) Biodegradation of naphthenic acids in oils sands process waters in an immobilized soil/sediment bioreactor. Chemosphere 109:164–172. https://doi.org/10.1016/j.chemosphere.2014.02.001

McMartin DW, Headley JV, Friesen DA et al (2004) Photolysis of naphthenic acids in natural surface water. J Environ Sci Health Part A 39:1361–1383. https://doi.org/10.1081/ESE-120037839

Medeiros DCCDS, Chelme-Ayala P, Gamal El-Din M (2023) Sorption and desorption of naphthenic acids on reclamation materials: mechanisms and selectivity of naphthenic acids from oil sands process water. Chemosphere 326:138462. https://doi.org/10.1016/j.chemosphere.2023.138462

Melvin SD, Trudeau VL (2012) Toxicity of naphthenic acids to wood frog tadpoles (*Lithobates sylvaticus*). J Toxicol Environ Health A Curr Issues 75:170–173. https://doi.org/10.1080/15287394.2012.640092

Morandi GD, Wiseman SB, Pereira A, Mankidy R, Gault IGM, Martin JW, Giesy JP (2015) Effects-directed analysis of dissolved organic compounds in Oil Sands Process-Affected Water. Environ Sci Technol 49:12395–12404. https://doi.org/10.1021/acs.est.5b02586

Natural Resources, Canada (2015) Oil sands, a strategic resource for Canada, North America and the global market. https://publications.gc.ca/pub?id=9.805605&sl=0

Philippot L, Raaijmakers JM, Lemanceau P, Van Der Putten WH (2013) Going back to the roots: the microbial ecology of the rhizosphere. Nat Rev Microbiol 11:789–799. https://doi.org/10.1038/nrmicro3109

Phillips LA, Armstrong SA, Headley JV, Greer CW, Germida JJ (2010) Shifts in root-associated microbial communities of *Typha latifolia* growing in naphthenic acids and relationship to plant health. Int J Phytoremediation 12:745–760. https://doi.org/10.1080/15226510903535106

Pietrangelo L, Bucci A, Maiuro L, Bulgarelli D, Naclerio G (2018) Unraveling the composition of the root-associated bacterial microbiota of *Phragmites australis* and *Typha latifolia*. Front Microbiol 9:1650. https://doi.org/10.3389/fmicb.2018.01650

Quinlan PJ, Tam KC (2015) Water treatment technologies for the remediation of naphthenic acids in oil sands process-affected water. Chem Eng J 279:696–714. https://doi.org/10.1016/j.cej.2015.05.062

R Core Team (2024) R: A language and environment for statistical computing

Reis MP, Ãvila MP, Costa PS, Barbosa FAR, Laanbroek HJ, Chartone-Souza E, Nascimento AMA (2014) The influence of human settlement on the distribution and diversity of iron-oxidizing bacteria belonging to the Gallionellaceae in tropical streams. Front Microbiol 5. https://doi.org/10.3389/fmicb.2014.00630

Reis PCJ, Correa-Garcia S, Tremblay J, Beaulieu-Laliberté A, Muench DG, Ahad JME, Yergeau E, Comte J, Martineau C (2023) Microbial degradation of naphthenic acids using constructed wetland treatment systems: metabolic and genomic insights for improved bioremediation of process-affected water. FEMS Microbiol Ecol 99:fiad153. https://doi.org/10.1093/femsec/fiad153

Roberts DW (1991) QSAR issues in aquatic toxicity of surfactants. Sci Total Environ 109–110:557–568. https://doi.org/10.1016/0048-9697(91)90209-W

Robinson CE, Elvidge CK, Frank RA, Headley JV, Hewitt LM, Little AG, Robinson SA, Trudeau VL, Vander Meulen IJ, Orihel DM (2023) Naphthenic acid fraction compounds reduce the reproductive success of wood frogs (*Rana sylvatica*) by affecting offspring viability. Environ Pollut 316:120455. https://doi.org/10.1016/j.envpol.2022.120455

Rodgers JH, Castle JW (2008) Constructed wetland systems for efficient and effective treatment of contaminated waters for reuse. Environ Geosci 15:1–8. https://doi.org/10.1306/eg.11090707019

Rogers VV, Wickstrom M, Liber K, MacKinnon MD (2002) Acute and subchronic mammalian toxicity of naphthenic acids from oil sands tailings. Toxicol Sci 66:347–355. https://doi.org/10.1093/toxsci/66.2.347

Rossoni S, Beard S, Segura-Bidermann MI, Duarte-Ramírez J, Osorio FK, Varas-Godoy M, Martínez-Bellange P, Vera M, Quatrini R, Castro M (2024) Membrane vesicles in Acidithiobacillia class extreme acidophiles: influence on collective behaviors of '*Fervidacidithiobacillus caldus*.' Front Microbiol 14:1331363. https://doi.org/10.3389/fmicb.2023.1331363

Scarlett AG, West CE, Jones D, Galloway TS, Rowland SJ (2012) Predicted toxicity of naphthenic acids present in oil sands process-affected waters to a range of environmental and human endpoints. Sci Total Environ 425:119–127. https://doi.org/10.1016/j.scitotenv.2012.02.064

Schultz JC, Appel HM, Ferrieri AP, Arnold TM (2013) Flexible resource allocation during plant defense responses. Front Plant Sci. 4https://doi.org/10.3389/fpls.2013.00324

Scott AC, Mackinnon MD, Fedorak PM (2005) Naphthenic acids in Athabasca Oil Sands tailings waters are less biodegradable than commercial naphthenic acids. Environ Sci Technol 39:8388–8394. https://doi.org/10.1021/es051003k

Scott AC, Zubot W, Davis CW, Brogly J (2020) Bioaccumulation potential of naphthenic acids and other ionizable dissolved organics in

oil sands process water (OSPW) – a review. Sci Total Environ 712:134558. https://doi.org/10.1016/j.scitotenv.2019.134558

Simair MC, Parrott JL, Le Roux M, Gupta V, Frank RA, Peru KM, Ajaero C, McMartin DW, Headley JV (2021) Treatment of oil sands process affected waters by constructed wetlands: evaluation of designs and plant types. Sci Total Environ 772:145508. https://doi.org/10.1016/j.scitotenv.2021.145508

Singer AC, Crowley DE, Thompson IP (2003) Secondary plant metabolites in phytoremediation and biotransformation. Trends Biotechnol 21:123–130. https://doi.org/10.1016/S0167-7799(02)00041-0

Stottmeister U, Wießner A, Kuschk P, Kappelmeyer U, Kästner M, Bederski O, Müller RA, Moormann H (2003) Effects of plants and microorganisms in constructed wetlands for wastewater treatment. Biotechnol Adv 22:93–117. https://doi.org/10.1016/j.biotechadv.2003.08.010

Syranidou E, Thijs S, Avramidou M, Weyens N, Venieri D, Pintelon I, Vangronsveld J, Kalogerakis N (2018) Responses of the endophytic bacterial communities of *Juncus acutus* to pollution with metals, emerging organic pollutants and to bioaugmentation with indigenous strains. Front Plant Sci 9:1526. https://doi.org/10.3389/fpls.2018.01526

Trepanier KE, Balaberda A, Vander Meulen IJ, Ahad JME, Correa-Garcia S, Morvan S, Bergeron M, Atugala D, Gieg L, Headley JV, Yergeau É, Martineau C, Degenhardt D (2025) Enhancing naphthenic acid attenuation in mesocosm wetlands: the role of temperature, plant species, and microbial communities. Water Environ Res. https://doi.org/10.1002/wer.70048

Trepanier KE, Vander Meulen IJ, Ahad JME, Headley JV, Degenhardt D (2023) Evaluating the attenuation of naphthenic acids in constructed wetland mesocosms planted with *Carex aquatilis*. Environ Monit Assess 195:1228. https://doi.org/10.1007/s10661-023-11776-8

Vähätalo AV, Wetzel RG (2008) Long-term photochemical and microbial decomposition of wetland-derived dissolved organic matter with alteration of 13 C:12 C mass ratio. Limnol Oceanogr 53:1387–1392. https://doi.org/10.4319/lo.2008.53.4.1387

Van Den Berg RA, Hoefsloot HC, Westerhuis JA, Smilde AK, Van Der Werf MJ (2006) Centering, scaling, and transformations: improving the biological information content of metabolomics data. BMC Genomics 7:142. https://doi.org/10.1186/1471-2164-7-142

Van den Heuvel MR, Hogan NS, Roloson SD, Van Der Kraak GJ (2012) Reproductive development of yellow perch (*Perca flavescens*) exposed to oil sands-affected waters. Environ Toxicol Chem 31:654–662. https://doi.org/10.1002/etc.1732

Vander Meulen IJ, Ahad JME, Martineau C, Muench DG, McMartin D, Headley JV (2025) Multi-Year Trends in the Spatiotemporal Occurrence and Fate of Naphthenic Acid Fraction Compounds in a Pilot-Scale. Engineered Treatment Wetland. https://doi.org/10.2139/ssrn.5194984

Vander Meulen IJ, Klemish JL, Peru KM, Yong Chen D, Pyle D, Headley GG, J.V (2021a) Molecular Profiles of Naphthenic Acid Fraction Compounds from Mine Lease Wetlands in the Athabasca Oil Sands Region. Chemosphere 129892. https://doi.org/10.1016/j.chemosphere.2021.129892

Vander Meulen IJ, Schock DM, Parrott JL, Mundy LJ, Pauli BD, Peru KM, McMartin DW, Headley JV (2021b) Characterization of naphthenic acid fraction compounds in water from Athabasca oil sands wetlands by Orbitrap high-resolution mass spectrometry. Sci Total Environ 780:146342. https://doi.org/10.1016/j.scitotenv.2021.146342

Verbeek AG (1995) A toxicity assessment of oil sands wastewater. National Library of Canada = Bibliothèque nationale du Canada, Ottawa

Whitby C (2022) A microbial solution to oil sand pollution: understanding the microbiomes, metabolic pathways and mechanisms involved in naphthenic acid (NA) biodegradation. In: Advances in ecological research. Elsevier, pp 231–287. https://doi.org/10.1016/bs.aecr.2022.10.001

Wießner A, Kuschk P, Stottmeister U (2002) Oxygen release by roots of *Typha latifolia* and *Juncus effusus* in laboratory hydroponic systems. Acta Biotechnol 22:209–216. https://doi.org/10.1002/1521-3846(200205)22:1/2%253C209::AID-ABIO209%253E3.0.CO;2-O

Woodcroft BJ, Aroney STN, Zhao R, Cunningham M, Mitchell JAM, Blackall L, Tyson GW (2024) SingleM and Sandpiper: Robust microbial taxonomic profiles from metagenomic data. https://doi.org/10.1101/2024.01.30.578060

Xie X, Yuan K, Yao Y, Sun J, Lin L, Huang Y, Lin G, Luan T, Chen B (2022) Identification of suspended particulate matters as the hotspot of polycyclic aromatic hydrocarbon degradation-related bacteria and genes in the Pearl River Estuary using metagenomic approaches. Chemosphere 286:131668. https://doi.org/10.1016/j.chemosphere.2021.131668

Zapata-Morales AL, Alfaro-De La Torre M, Hernández-Morales A, García-De La Cruz RF (2020) Isolation of cultivable bacteria associated with the root of *Typha latifolia* in a constructed wetland for the removal of diclofenac or naproxen. Water Air Soil Pollut 231:423. https://doi.org/10.1007/s11270-020-04781-x

Zerveas S, Mente MS, Tsakiri D, Kotzabasis K (2021) Microalgal photosynthesis induces alkalization of aquatic environment as a result of H+ uptake independently from CO2 concentration – new perspectives for environmental applications. J Environ Manage 289:112546. https://doi.org/10.1016/j.jenvman.2021.112546

Zhang L, Zhang Y, Gamal El-Din M (2019) Integrated mild ozonation with biofiltration can effectively enhance the removal of naphthenic acids from hydrocarbon-contaminated water. Sci Total Environ 678:197–206. https://doi.org/10.1016/j.scitotenv.2019.04.302

Zhang N, A D, Chao Y, Li H-Y, Li C, Lin Q, Li Y, Qiu R (2023) Mechanism of polycyclic aromatic hydrocarbons degradation in the rhizosphere of *Phragmites australis*: organic acid co-metabolism, iron-driven, and microbial response. Environ Pollut 327:121608. https://doi.org/10.1016/j.envpol.2023.121608

Zhao Y, Naeth MA, Wilkinson SR, Dhar A (2024) Phytoremediation of metals in oil sands process affected water by native wetland species. Ecotoxicol Environ Saf 282:116732. https://doi.org/10.1016/j.ecoenv.2024.116732

Zheng Y, Su F, Li H, Song F, Wei C, Cui P (2024) Structure and function of soil bacterial communities in the different wetland types of the Liaohe Estuary Wetland. Microorganisms 12:2075. https://doi.org/10.3390/microorganisms12102075

Zheng Y, Tan Y, Wan Z, Zhang P, Li X, Yuan S (2025) Carbon isotope fractionation of dissolved organic matter due to $^{\bullet}$OH-based oxidation. Environ Sci Technol 59:9104–9112. https://doi.org/10.1021/acs.est.5c01310

Zuur AF, Ieno EN, Elphick CS (2010) A protocol for data exploration to avoid common statistical problems. Methods Ecol Evol 1:3–14. https://doi.org/10.1111/j.2041-210x.2009.00001.x

Publisher's Note Springer Nature remains neutral with regard to jurisdictional claims in published maps and institutional affiliations.